Insulin-like growth factor binding protein-2 in at-risk adults and autopsy-confirmed Alzheimer brains

Marc James Quesnel,[1,2] Anne Labonté,[2,3] Cynthia Picard,[2,3] Henrik Zetterberg,[4,5,6,7,8,9] Kaj Blennow,[4,5,10,11] Ann Brinkmalm,[4,5] Sylvia Villeneuve[1,2,3] and Judes Poirier[1,2,3] for the Alzheimer's Disease Neuroimaging Initiative and the PREVENT-AD Research Group

Abstract

Insulin, insulin-like growth factors (IGF) and their receptors are highly expressed in the adult hippocampus. Thus, disturbances in the insulin-IGF signaling pathway may account for the selective vulnerability of the hippocampus to nascent Alzheimer's disease (AD) pathology. In the present study, we examined the predominant IGF-binding protein (IGFBP) in the cerebrospinal fluid (CSF) – IGFBP2.

CSF was collected from 109 asymptomatic members of the parental history-positive PREVENT-AD cohort. CSF levels of IGFBP2, core AD biomarkers and synaptic biomarkers were measured using proximity extension assay, ELISA and mass spectrometry. Cortical amyloid-beta (Aβ) and tau deposition were examined using ^{18}F-NAV4694 and flortaucipir. Cognitive assessments were performed up to 8 years of follow-up, using the Repeatable Battery for the Assessment of Neuropsychological Status. T1-weighted structural MRI scans were acquired, and neuroimaging analyses were performed on pre-specified temporal and parietal brain regions. Next, in an independent cohort, we allocated 241 dementia-free ADNI-1 participants into four stages of AD progression based on the biomarkers CSF $A\beta_{42}$ and total-tau (t-tau). In this analysis, differences in CSF and plasma IGFBP2 levels were examined across the pathological stages. Finally, IGFBP2 mRNA and protein levels were examined in the frontal cortex of 55 autopsy-confirmed AD and 31 control brains from the QFP cohort, a unique population isolate from Eastern Canada.

CSF IGFBP2 progressively increased over 5 years in asymptomatic PREVENT-AD participants. Baseline CSF IGFBP2 was positively correlated with CSF AD biomarkers and synaptic biomarkers, and was negatively correlated with longitudinal changes in delayed memory ($P = 0.024$) and visuospatial abilities ($P = 0.019$). CSF IGFBP2 was negatively correlated at a trend-

level with entorhinal cortex volume ($P = 0.082$) and cortical thickness in the piriform ($P = 0.039$), inferior temporal ($P = 0.008$), middle temporal ($P = 0.014$) and precuneus ($P = 0.033$) regions. In ADNI-1, CSF ($P = 0.009$) and plasma ($P = 0.001$) IGFBP2 were significantly elevated in Stage 2 (CSF Aβ(+)/t-tau(+)). In survival analyses in ADNI-1, elevated plasma IGFBP2 was associated with a greater rate of AD conversion (HR = 1.62, $P = 0.021$). In the QFP cohort, IGFBP2 mRNA was reduced ($P = 0.049$), however IGFBP2 protein levels did not differ in the frontal cortex of autopsy-confirmed AD brains ($P = 0.462$).

Nascent AD pathology may induce an upregulation in IGFBP2, in asymptomatic individuals. CSF and plasma IGFBP2 may be valuable markers for identifying CSF Aβ(+)/t-tau(+) individuals and those with a greater risk of AD conversion.

Author affiliations:

1 McGill University, Department of Psychiatry, Montréal, Québec, Canada, H3A 1A1

2 Douglas Mental Health University Institute, Research Centre, Montréal, Québec, Canada, H4H 1R3

3 Centre for the Studies in the Prevention of Alzheimer's Disease, Douglas Mental Health University Institute, Montréal, Québec, Canada, H4H 1R3

4 Department of Psychiatry and Neurochemistry, Institute of Neuroscience and Physiology, The Sahlgrenska Academy, University of Gothenburg, Gothenburg, Sweden

5 Clinical Neurochemistry Department, Sahlgrenska University Hospital, Mölndal, Sweden

6 Department of Neurodegenerative Disease, UCL Institute of Neurology, London, WC1N 3BG, UK

7 UK Dementia Research Institute at UCL, London, WC1E 6BT, UK

8 Hong Kong Center for Neurodegenerative Diseases, Hong Kong, China

9 Wisconsin Alzheimer's Disease Research Center, University of Wisconsin School of Medicine and Public Health, University of Wisconsin-Madison, Madison, WI 53792-2420 USA

2

1 10 Paris Brain Institute, ICM, Pitié-Salpêtrière Hospital, Sorbonne University, 21 414 – 75646

2 Paris Cedex 13, Paris, France

3 11 Neurodegenerative Disorder Research Center, Division of Life Sciences and Medicine, and

4 Department of Neurology, Institute on Aging and Brain Disorders, University of Science and

5 Technology of China and First Affiliated Hospital of USTC, Hefei, P.R. China

6

7 Correspondence to: Dr Judes Poirier

8 Centre for the Studies in the Prevention of Alzheimer's Disease, Douglas Mental Health University

9 Institute, 6875, Lasalle, Montréal, Quebec H4H 1R3, Canada

10 E-mail: judes.poirier@mcgill.ca

11 **Running title**: Role of IGFBP2 across the AD spectrum

12

RBANS, Repeatable Battery for the Assessment of Neuropsychological Status; ROI, region of interest; Rpm, revolutions per minute; SHANK3, SH3 And Multiple Ankyrin Repeat Domains 3; SNAP, suspected non-Alzheimer pathology; SNAP25, synaptosomal-associated protein 25; SUVR, standardized uptake value ratio; SYT1, synaptotagmin-1; t-tau: total tau

Introduction

By 2050, is it estimated that 152.8 million individuals worldwide will be affected by dementia.[1] Furthermore, the cost of dementia care is projected to reach \$16.9 trillion in 2050.[2] Alzheimer's disease (AD) remains one of the most challenging medical mysteries, as it is the most common cause of dementia - accounting for 60-80% of all cases.[3] The neuropathological hallmarks of AD include the accumulation of extracellular amyloid-beta (Aβ) plaques, intracellular neurofibrillary tangles, as well as the loss of synapses and neurons.[4] These brain changes are believed to begin up to 20 years or more, before the onset of symptoms.[5]

It has been well established that insulin resistance and diabetes are risk factors for developing AD.[6,7] Indeed, impaired insulin and insulin-like growth factor (IGF) signalling plays a critical role in the pathogenesis of AD.[8-10] Post-mortem studies have demonstrated that insulin, IGFs as well as their receptors and downstream signalling molecules, are decreased in the AD brain.[8-11] Furthermore, the insulin-IGF system has been shown to directly modulate Aβ degradation[12] and clearance,[13] phospho-tau production,[14,15] synaptic integrity[16] and neuronal survival.[17] It is also known that insulin, IGFs and their receptors are highly expressed in the hippocampus, relative to the frontal cortex in the human brain.[8] Overall, these findings suggest that impairments in insulin-IGF signaling may account for the selective vulnerability of the hippocampus to nascent AD pathology, and therefore, account for early impairments in episodic memory. Similarly, deficiencies in insulin-IGF signaling may contribute to the reductions in glucose metabolism that are seen in patients with AD and individuals at risk for AD.[18] The importance of insulin and IGFs has been emphasized in pilot clinical trials in which the administration of intranasal insulin improved memory, caregiver-rated functional abilities, and glucose metabolism in individuals with mild cognitive impairment (MCI) or mild AD.[19,20]

The insulin-IGF system encompasses a complex collection of proteins that play pivotal roles in glucose metabolism, neurogenesis, synaptogenesis and cell survival.[17,21,22] Insulin, IGF-I and IGF-II are the key proteins, which bind to their cell surface receptors.[22] The actions of IGF-I and IGF-II are modulated by six IGF-binding proteins (IGFBP), which can bind to IGFs with an equal or greater affinity than the IGF receptors.[23,24] Indeed, in the circulation, CSF and local tissues, most extracellular IGFs are bound to so-called IGFBPs, which prolong the half-life of IGFs.[22-24] For instance, it has been proposed that IGFBPs may prevent the degradation of IGFs during transport and mobilisation, and target IGFs to their receptors.[22-24] The latter may be achieved through IGFBPs binding to cell-surface proteoglycans[25] and integrins,[26] or proteolytic cleavage,[27] both of which reduce the binding affinity of IGFBPs for IGFs and promote IGF release.[22]

The main objective of the current study is to examine a less studied member of the IGF molecular cascade, insulin-like growth factor binding protein-2 (IGFBP2), in both the pre-symptomatic and symptomatic stages of AD. Since IGFBP2 is the most abundant IGF-binding protein in the CSF,[28,29] we hypothesize IGFBP2 plays a critical role in the neurodegenerative process, most likely at the level of neuroprotection and resilience.[22] IGFBP2 is increased in the CSF and plasma of patients with a clinical diagnosis of AD,[30-35] and is associated with longitudinal atrophy in entorhinal, parahippocampal and inferior temporal regions.[36] Moreover, elevated circulating levels of IGFBP2 have been associated with an increased risk of developing AD.[35,37,38] Finally, in a pilot study, IGFBP2 has been found to be decreased in the temporal cortex of AD patients.[9] These and other findings will be verified in the pre-symptomatic and symptomatic stages of the disease, as well as in autopsy-confirmed AD brains.

Materials and methods

PREVENT-AD cohort

Study participants

The PRe-symptomatic EValuation of Experimental or Novel Treatments for Alzheimer's Disease (PREVENT-AD) cohort consists of asymptomatic, "at-risk", individuals with a parental or multi-sibling history of sporadic Alzheimer's disease.[39] The majority of participants were over the age

1   of 60, however individuals aged 55-59 years were included if they were within 15 years of the

2   onset of their youngest-affected relative's symptoms. In order to confirm normal cognition, the

3   Clinical Dementia Rating and Montreal Cognitive Assessment (MoCA) were used at the study

4   eligibility visit. 386 active PREVENT-AD participants have been followed longitudinally, as

5   annual visits include cognitive assessments, neurosensory tests, blood and (for a subset of

6   individuals) CSF collections, structural and functional MRI scans, as well as PET scans. Each

7   participant and their study partner provided written informed consent. All procedures were

8   approved by the McGill University Faculty of Medicine Institutional Review Board and complied

9   with the ethical principles of the Declaration of Helsinki. A detailed description of the PREVENT-

10   AD cohort is available elsewhere.[39]

11

Cerebrospinal fluid measurements

13   A Sprotte 24-gauge atraumatic needle was used to perform lumbar punctures (LP) in PREVENT-

14   AD participants, following an overnight fast. In order to exclude cells and insoluble material, CSF

15   samples were centrifuged (~2000g) within 4 hours, for 10 minutes at room temperature. Finally,

16   the CSF samples were aliquoted (0.5 mL) into polypropylene cryotubes and stored at -80°C.

17   CSF IGFBP2 levels were measured in a subset of PREVENT-AD participants ($n = 109$) using the

18   Olink Cardiovascular III panel (Uppsala, Sweden), which employs proximity extension assay

19   technology. Olink measurements are expressed in arbitrary Normalized Protein eXpression units

20   (NPX), which are on a $\log_2$ scale.

21   CSF AD biomarkers amyloid-beta 42 ($A\beta_{42}$), phosphorylated tau (p_{181}-tau) and total tau (t-tau)

22   were measured in a subset ($n = 101$) of PREVENT-AD participants, using the validated Innotest

23   ELISA kit (Fujirebio, Ghent, Belgium) following the standardized protocols established by the

24   BIOMARKAPD consortium ($A\beta_{42}$ Cat.# 81583, p_{181}-tau Cat.# 81581 and t-tau Cat.# 81579).

25   Of the 109 PREVENT-AD participants that had CSF IGFBP2 measurements, 106 individuals had

26   the synaptic proteins synaptosomal-associated protein 25 (SNAP25) and synaptotagmin-1 (SYT1)

27   assayed. CSF SNAP25 and SYT1 were immunoprecipitated and their concentrations were

28   determined by mass spectrometry, as previously described.[40,41,42] Mass spectrometry results are

29   expressed in arbitrary units.[43] As previously reported, CSF levels of growth-associated protein 43

(GAP43) and neurogranin (NRGN) were assessed by validated ELISAs in a subset of PREVENT-AD individuals ($n = 46$).[44,45]

Neuroimaging acquisition and processing

In vivo cortical Aβ and phosphorylated tau pathologies were determined using PET tracers ^{18}F-NAV4694 (Navidea Biopharmaceuticals, Dublin, OH, USA) and flortaucipir (^{18}F-AV1451; Eli Lilly & Company, Indianapolis, IN, USA), in a subset of PREVENT-AD participants that also had CSF IGFBP2 measurements ($n = 46$, $n = 49$ respectively). Aβ and tau PET scans were performed 40 to 70 minutes and 80 to 100 minutes post-injection, respectively. A 3T Siemens Trio scanner was used to acquire T1-weighted structural MRI scans at the Douglas Mental Health University Institute (Montreal). A Siemens standard 12 or 32-channel coil was used (Siemens Medical Solutions, Erlangen). FreeSurfer 5.3 was used to process the MRI scans, and the Desikan-Killiany atlas was used for parcellation. The preprocessing pipeline for PET images has previously been described.[46] Briefly, standardized uptake value ratios (SUVRs) were generated by dividing the signal in the regions of interest (ROI) by the signal in the reference region. Thus, cerebellar grey matter was used as a reference region for ^{18}F-NAV4694, whilst the inferior cerebellar grey matter was used for flortaucipir. A global cortical ROI was computed to evaluate Aβ deposition, whilst tau deposition was assessed by averaging flortaucipir SUVRs in the entorhinal cortex and lingual gyri. The imaging processing pipeline CIVET 1.1.12 was used to estimate cortical thickness from T1-weighted images ($n =104$).[47] Brain volumes were computed using a volumetric pipeline that has been previously described.[48]

Apolipoprotein E genotyping

The QIAsymphony apparatus and DNA Blood Mini QIA Kit were used to isolate DNA from 200 ul whole blood (Qiagen, Valencia, CA, USA). The standard QIASymphony isolation program was used following the manufacturer's instructions. The PyroMark Q96 pyrosequencer (Qiagen, Toronto, Ontario, Canada) was used to determine apolipoprotein E (APOE) genotype in PREVENT-AD. qPCR was used to amplify DNA, with primers rs429358 amplification forward 5'-ACGGCTGTCCAAGGAGCTG-3', rs429358 amplification reverse biotinylated 5'-

7

CACCTCGCCGCGGTACTG-3', rs429358 sequencing 5'CGGACATGGAGGACG-3', rs7412

amplification forward 5'-CTCCGCGATGCCGATGAC-3', rs7412 amplification reverse

biotinylated 5'-CCCCGGCCTGGTACACTG-3' and rs7412 sequencing 5'-CGA

TGACCTGCAGAAG-3'.

Cognitive testing

At annual visits, the Repeatable Battery for the Assessment of Neuropsychological Status
(RBANS) was used to assess the cognitive performance of PREVENT-AD participants. The
RBANS possesses an excellent sensitivity in differentiating normal cognition from MCI.[49] Five
cognitive domains are evaluated, which include immediate memory, delayed memory, attention,
language and visuospatial abilities.[49] A total summary score is included as well. Each participant's
score is standardized by their age, such that a score of 100 represents the expected cognitive
performance for a given age.[49] In order to reduce practice effects in longitudinal assessment, the
RBANS was available in four equivalent versions. Furthermore, the battery was administered in
English or French depending on the participants' preferred language. Cognitive measurements are
available for up to 8 years of follow-up.

ADNI-1 cohort

Study participants

Led by Principal Investigator Michael W. Weiner, MD, the primary objective of the Alzheimer's
Disease Neuroimaging Initiative (ADNI) has been to detect the earliest changes associated with
AD, and to track the progression of AD pathology. Given our interest in the earliest possible stages
of AD, we restricted our primary analyses to 241 ADNI-1 participants with CSF data available
from 92 cognitively unaffected (CU) individuals and 149 individuals with MCI. For analyses
involving plasma samples, we restricted our analyses to 58 CU individuals and 396 individuals
with MCI that had available data. Two individuals with ambiguous diagnoses were excluded from
analyses.

8

Cerebrospinal fluid measurements

LPs were performed with a 20- or 24- gauge spinal needle, following an overnight fast. CSF samples were frozen within 1 hour after collection and shipped on dry ice to the ADNI Biomarker Core laboratory. Following thawing (1h) with gentle mixing at room temperature, the samples were aliquoted (0.5 mL) into polypropylene vials and stored at -80°C. CSF AD biomarkers $A\beta_{42}$, p_{181}-tau and t-tau were measured in ADNI-1 samples using the INNO-BIA AlzBio3 immunoassay kits (Fujirebio, Ghent, Belgium) and the xMap Luminex platform (Austin, Texas, USA).

CSF levels of 159 inflammatory, metabolic and lipid analytes, including IGFBP2 had been assessed with the Human Discovery Map panel, a multiplex immunoassay panel developed by Rules Based Medicine. In the case of IGFBP2, 8 (imputed) samples exceeded the detectable analyte concentration range and were omitted from subsequent analyses. Finally, in supplementary analyses, we further analyzed multiple reaction monitoring mass spectrometry measurements of CSF IGFBP2.

Pathological staging of participants

Following the recent emergence of biological frameworks for defining AD,[50] we used baseline CSF $A\beta_{42}$ and CSF t-tau measurements to stage 90 CU individuals and 145 individuals with MCI. We applied the recommended CSF $A\beta_{42}$ and CSF t-tau thresholds of <192 pg/mL and >93 pg/mL, respectively.[51] These cutoff values have been generated from autopsy-based AD CSF samples and have been reported to detect mild AD and predict the conversion from MCI to AD.[51] Two individuals with biomarker measurements equivalent to the threshold values were removed.

ADNI-1 participants were assigned to Stage 0, $A\beta$(-)/t-tau(-), if they had normal levels of CSF $A\beta_{42}$ and CSF t-tau. Participants in Stage 1, $A\beta$(+)/t-tau(-), exhibited early amyloid pathology, as reflected by reduced levels of CSF $A\beta_{42}$. However, individuals in Stage 1 did not display significant levels of neuronal loss, as reflected by low levels of CSF t-tau. In Stage 2, $A\beta$(+)/t-tau(+), participants exhibited low levels of CSF $A\beta_{42}$ and elevated levels of CSF t-tau. Finally, the Suspected Non-Alzheimer Pathology (SNAP) group, $A\beta$(-)/t-tau(+), exhibited normal levels of CSF $A\beta_{42}$ and elevated levels of CSF t-tau, thus suggesting other causes of neurodegeneration and/or dementia.

Plasma measurements

At the baseline visit, plasma samples were drawn following an overnight fast. 192 analytes that have been reported to be altered in cancer, cardiovascular disease, metabolic disorders, inflammation and AD were analyzed with the Human Discovery Map panel, a multiplex immunoassay panel developed on the Luminex xMAP platform by Rules Based Medicine. In order to meet model assumptions, plasma IGFBP2 levels were $\log_{10}$ transformed by the ADNI investigators.

Apolipoprotein E genotyping

The ABI 7900 real-time thermo-cycler (Applied Biosystems, Foster City, CA) was used to determine the APOE genotype of ADNI participants. TaqMan qPCR was applied to DNA prepared from EDTA whole blood.

QFP cohort

Study participants

The Quebec Founder Population (QFP) is composed of the descendants of a few thousand French settlers that colonized Nouvelle France in the 17th and 18th centuries.[52] The migration and the isolated nature of settlements created a founder effect, which resulted in a population with less genetic heterogeneity.[52] Genealogical information for this population, for almost four centuries, is available in the BALSAC database. In the present study, we analyzed the brains of 55 autopsy-confirmed AD cases and 31 autopsy-confirmed elderly controls, which were obtained from the Douglas-Bell Canada Brain Bank. According to medical record reviews, neuropsychological examinations and caregiver interviews, there was no evidence of memory problems, neurological or neuropsychiatric diseases in the elderly control group. Furthermore, controls only exhibited neuropathology that is associated with healthy aging (plaque and tangle densities <10/mm^3 and < 20/mm^3 in at least one hippocampal and neocortical section). AD cases had to fulfill the histopathological NINCDS-ADRDA criteria for definite AD.[53] This study was conformed to the Code of Ethics of the World Medical Association and was approved by the Ethics Board of the

Douglas Mental Health University Institute. This study complied with the ethical principles of the Declaration of Helsinki. Each participant provided written informed consent.

IGFBP2 gene expression in the frontal cortex

In the frontal cortex of 31 autopsy-confirmed controls and 55 autopsy-confirmed AD cases, transcriptome-wide gene expression was measured using the human Clariom D Assay, by Génome Québec. Briefly, the Nanodrop Spectrophotometer ND-1000 was used to measure total RNA (NanoDrop Technologies, Inc.). RNA integrity was evaluated with the Agilent 2100 Bioanalyzer. 10 ng of total RNA was used to synthesize sense-strand cDNA. The GeneChip WT Terminal Labeling Kit was used to fragment and label single-stranded cDNA, following the manufacture's instructions. 5 µg cDNA was hybridized on the GeneChip cartridge array and incubated at 45°C for 17 hours in the GeneChip Hybridization Oven 640, at 60 rpm. The microarrays were washed in the GeneChip Fluidics Station 450, using the GeneChip Hybridization, Wash, and Stain Kit, according to the manufacture's instructions. Finally, microarrays were scanned in a GeneChip Scanner 3000. IGFBP2 mRNA levels are presented on a $\log_2$ scale.

IGFBP2 protein levels in the frontal cortex

Of the 86 brains that had IGFBP2 mRNA levels measured, 78 brains ($n = 25$ Controls, $n = 53$ AD) had IGFBP2 protein levels measured. Frontal cortex brain samples were placed in pre-filled tubes containing 2.8 mm ceramic beads (Omni International, GA, USA). One tablet of protease inhibitor was dissolved in 50 mL of cold phosphate-buffered saline. 1 mL of protease inhibitor solution was added to each tube. The Bead Ruptor 24 (Omni International, Kennesaw, GA, USA) was used to mechanically homogenize brain samples. The Bead Ruptor 24 was set twice at 5.65m/s for 30 seconds, with a 15 second pause between runs. Following homogenization, the samples were stored overnight at -20°C. In order to break the cell membranes, two freeze-thaw cycles were performed. Finally, the homogenates were centrifuged for 5 minutes at 5000 rpm and 4°C. The supernatant was collected and stored for future use at -80°C.

Frontal cortex IGFBP2 protein levels were measured using a commercially available ELISA kit (Cat.# OKEH00084, Aviva Systems Biology, CA, USA). Protocols were performed according to

11

1 the manufacturers' instructions and results were obtained using the BioTek Synergy H1 microplate

2 reader (Winooski, Vermont, USA). Sample replicates had a coefficient of variability of less than

3 20%. Finally, in order to normalize IGFBP2 protein levels, total protein concentration was

4 measured using a commercially available bicinchoninic acid assay developed by Pierce (Cat.#

5 23225). Finally, normalized IGFBP2 protein ratios were $\log_2$ transformed in order to meet model

6 assumptions.

7

Apolipoprotein E genotyping

9 DNA was extracted from brain tissue with the DNeasy Tissue Kit (Qiagen). As previously

10 described in PREVENT-AD,[39] the PyroMark Q96 pyrosequencer was used to determine *APOE*

11 genotype.

12

Statistical analyses

14 Annual changes in CSF IGFBP2 levels were assessed in a subset of PREVENT-AD participants

15 ($n = 27$). Each participant's trajectory was analyzed using a linear mixed model with a random

16 intercept and slope. Age, sex and *APOE* ε4 carrier status – adjusted linear regression models were

17 used to examine the associations between baseline CSF IGFBP2 and baseline measurements of

18 CSF AD biomarkers (Aβ_{42}, p$_{181}$-tau, t-tau), CSF synaptic proteins (SYT1, SNAP25, GAP43,

19 NRGN) as well as PET and structural (volumetric, cortical thickness) neuroimaging data. For each

20 PREVENT-AD participant that was followed for 5-8 years ($n = 89$), an estimated cognitive

21 performance trajectory slope was calculated for each of the five cognitive domains of the RBANS.

22 Thus, linear regression models adjusted for age, sex, *APOE* ε4 carrier status and years of education

23 were used to examine the relationship between rate of change in cognition and baseline CSF

24 IGFBP2 levels. Across all analyses, IGFBP2 was assigned as a dependent variable, except for the

25 association with CSF Aβ_{42}. Finally, given the critical role of the insulin-IGF system in diverse

26 metabolic processes, we further controlled for clinical covariates such as body mass index (BMI),

27 systolic blood pressure and hemoglobin A1C levels (HbA1c), in supplementary analyses.

28 However, the results of these analyses were similar to those of the original model. Therefore, the

29 following results are presented according to the original model.

12

1 In the ADNI-1 cohort, analysis of covariance (ANCOVA) was used to assess the relationship

2 between baseline CSF and baseline plasma IGFBP2 with pathological stage as determined by CSF

3 Aβ_{42} and CSF t-tau positivity.[50,51] To correct for multiple planned comparisons between

4 pathological stages, statistical significance was considered at $P \leq 0.01$. Finally, Cox proportional

5 hazards models examined the association between baseline plasma IGFBP2 levels and rate of

6 conversion to AD. CU participants and individuals with MCI were followed from the baseline visit

7 to the time of diagnosis (of AD), or to the time the participant was last confirmed to be free of AD.

8 Cox models were adjusted for age, gender and *APOE* ε4 carrier status.

9 In the QFP cohort, the relationship between frontal cortex mRNA, protein levels, and diagnosis

10 was evaluated with ANCOVA adjusted for age at death, sex, *APOE* ε4 carrier status and post-

11 mortem delay. Statistical significance was considered at $P \leq 0.05$. R^2 values are presented as

12 adjusted R^2. All Analyses were two-tailed and performed in SPSS 23 (IBM) and JMP Pro 16

13 (SAS).

14

15 # Results

16 ## Demographics

17 Table 1 summarizes the demographic characteristics of the three cohorts that were used to analyze

18 the role of IGFBP2 in the CSF of asymptomatic (PREVENT-AD) and symptomatic individuals

19 (ADNI-1), as well as in the frontal cortex of autopsy-confirmed, age-matched control and AD

20 cases (QFP).

21

22 ## PREVENT-AD cohort

23 ### CSF IGFBP2 increases annually and is associated with CSF and PET

24 ### biomarkers in asymptomatic AD

25 In a subset of CU PREVENT-AD participants that had longitudinal CSF IGFBP2 measurements

26 available ($n = 27$), a random intercept and random slope linear mixed model revealed that CSF

27 IGFBP2 levels progressively increase over the course of five years ($\beta = 0.132$, $P = 0.005$, Fig. 1).

In PREVENT-AD participants ($n = 101$) that had CSF AD pathological biomarker measurements, baseline CSF IGFBP2 levels were positively correlated with CSF $A\beta_{42}$ ($R^2 = 0.055$, $\beta = 91.232$, $P = 0.023$, Fig. 2A), CSF p_{181}-tau ($R^2 = 0.162$, $\beta = 0.014$, $P = 4.50 \times 10^{-5}$, Fig. 2B) and CSF t-tau ($R^2 = 0.121$, $\beta = 0.001$, $P = 0.001$, Fig. 2C). In a subset of PREVENT-AD participants that underwent $A\beta$ and tau PET scans ($n = 46$ and $n = 49$), CSF IGFBP2 was not associated with global cortical $A\beta$ deposition ($P = 0.540$, Fig. 2D). However, CSF IGFBP2 was positively correlated (trend-level) with tau deposition in the entorhinal cortex ($R^2 = 0.027$, $\beta = 1.498$, $P = 0.082$, Fig. 2E) and lingual gyrus ($R^2 = 0.034$, $\beta = 2.226$, $P = 0.067$, Supplementary Fig. 1).

Finally, CSF IGFBP2 was positively associated with synaptic proteins in the CSF, including SNAP25 (trend-level, $R^2 = 0.051$, $\beta = 0.014$, $P = 0.076$, Fig. 2F), SYT1 ($R^2 = 0.060$, $\beta = 0.008$, $P = 0.043$, Fig. 2G), GAP43 ($R^2 = 0.243$, $\beta = 3.06 \times 10^{-4}$, $P = 2.52 \times 10^{-4}$, Fig. 2H), and NRGN (trend-level, $R^2 = 0.033$, $\beta = 0.002$, $P = 0.063$, Fig. 2I).

CSF IGFBP2 is linked to changes in delayed memory and visuospatial abilities in asymptomatic AD

Upon computing RBANS cognitive performance trajectory slopes estimated over the course of 5 to 8 years in a subset of PREVENT-AD participants ($n = 89$), baseline CSF IGFBP2 levels were negatively correlated with estimated rates of change in delayed memory scores ($R^2 = 0.072$, $\beta = -0.098$, $P = 0.024$, Fig. 3). Furthermore, baseline CSF IGFBP2 levels were negatively correlated with rates of change in visuospatial constructional abilities ($R^2 = 0.077$, $\beta = -0.082$, $P = 0.019$, Fig. 3). However, baseline IGFBP2 levels were not associated with changes in immediate memory ($P = 0.191$), language ($P = 0.332$) or attention ($P = 0.679$) (data not shown).

CSF IGFBP2 is associated with cortical atrophy in AD-specific brain regions in asymptomatic AD

We analyzed baseline structural neuroimaging data collected from a subset of PREVENT-AD individuals ($n = 104$) in a cross-sectional fashion. Four individuals were omitted from analyses due to failed quality control regarding subject-specific stereotaxic registration and/or brain

14

masking. After adjusting for total intracranial volume (ICV), baseline CSF IGFBP2 was negatively correlated with entorhinal cortex volumes in the left hemisphere at a trend-level ($R^2 = 0.117$, $\beta = -39.720$, $P = 0.082$, Fig. 4A). However, CSF IGFBP2 was not associated with entorhinal cortex volume in the right hemisphere ($P = 0.962$).

Next, we analyzed baseline cortical thickness in pre-specified temporal and parietal brain regions that are vulnerable to early AD pathology. Baseline CSF IGFBP2 was found to be negatively correlated with cortical thickness in the piriform cortex (trend, left hemisphere: $R^2 = 0.121$, $\beta = -0.628$, $P = 0.064$; right hemisphere: $R^2 = 0.128$, $\beta = -0.709$, $P = 0.039$, Fig. 4B), inferior temporal gyrus (left hemisphere: $R^2 = 0.153$, $\beta = -1.253$, $P = 0.008$; right hemisphere: $P = 0.315$, Fig. 4C), middle temporal gyrus (left hemisphere: $R^2 = 0.144$, $\beta = -1.369$, $P = 0.014$; right hemisphere: $R^2 = 0.116$, $\beta = -0.959$, $P = 0.090$, Fig. 4D), and precuneus (left hemisphere: $P = 0.123$; right hemisphere: $R^2 = 0.131$, $\beta = -1.353$, $P = 0.033$, Supplementary Fig. 2).

Changes in CSF IGFBP2 are not caused by alterations of the blood brain barrier integrity in asymptomatic subjects

To examine possible blood-brain barrier (BBB) dysfunction and possible peripheral vascular contributions to CSF IGFBP2 levels, we measured microprotein levels, red blood cell count and white blood cell count in the CSF. We did not find any associations between these vascular factors and CSF IGFBP2 (Supplementary Fig. 3); consistent with a relatively intact BBB in asymptomatic PREVENT-AD participants.[54]

ADNI-1 cohort

CSF and plasma IGFBP2 concentrations are elevated in CSF Aβ(+)/t-tau(+) individuals

89 CU individuals and 144 individuals with MCI from ADNI were staged as amyloid and/or tau positive according to recommended CSF Aβ$_{42}$ and CSF t-tau thresholds of 192 pg/mL and 93 pg/mL, respectively (Fig. 5A).[50,51] The results from the CSF multiplex immunoassay (Fig. 5B) revealed that baseline CSF IGFBP2 levels did not differ between Stages 0 ($n = 80$) Aβ(-)/t-tau(-)

15

1 and Stage 1 ($n = 68$) Aβ(+)/t-tau(-), $P = 0.541$. However, CSF IGFBP2 was significantly elevated

2 at Stage 2 ($n = 77$) Aβ(+)/t-tau(+) relative to Stage 0 ($P = 0.009$) and Stage 1 ($P = 0.001$). Finally,

3 CSF IGFBP2 was significantly increased in SNAP ($n = 8$) Aβ(-)/t-tau(+), relative to Stage 0 ($P =$

4 0.010).

5 To reproduce our findings, we performed replication analyses using CSF mass spectrometry data

6 acquired from a subset of the same ADNI participants. These supplementary analyses revealed

7 that both CSF IGFBP2 peptides, HGLYNLK (Supplementary Fig. 4) and LIQGAPTIR

8 (Supplementary Fig. 5) were significantly reduced at Stage 1 ($n = 62$) relative to Stage 0 ($n = 75$),

9 $P = 0.005$ and $P = 0.051$ (trend). Although a similar reduction at Stage 1 was observed with the

10 multiplex immunoassay data, it was not statistically significant. However, similar to the multiplex

11 immunoassay data, both IGFBP2 peptides were significantly elevated at Stage 2 ($n = 72$) relative

12 to Stage 1, $P = 1.50 \times 10^{-5}$ and $P = 2.21 \times 10^{-4}$. Likewise, both IGFBP2 peptides were markedly

13 increased in SNAP ($n = 9$) relative to Stage 0, $P = 4.90 \times 10^{-5}$ and $P = 0.002$, consistent with the

14 immunoassay results.

15 Finally, we staged 58 CU individuals and 196 individuals with MCI from ADNI, that had both

16 baseline plasma IGFBP2 measurements and CSF Aβ$_{42}$ and CSF t-tau measurements (Fig. 5C).

17 Baseline plasma IGFBP2 levels were significantly elevated in Stage 2 ($n = 84$) relative to Stage 0

18 ($n = 98$), $P = 0.001$, and to Stage 1 ($n = 60$), $P = 0.041$ (trend). However, plasma IGFBP2 did not

19 differ between Stage 0 and Stage 1 ($P = 0.208$), or between Stage 0 and SNAP ($n = 12$), $P = 0.874$.

20

21 **Elevated plasma IGFBP2 is associated with a faster rate of conversion to AD**

22 In the primary analysis for conversion to AD in ADNI, we established baseline plasma IGFBP2

23 threshold values at the 25th percentile (≤1.83251, first quartile, log$_{10}$ transformed) and above the

24 75th percentile (≥2.09342, fourth quartile, log$_{10}$ transformed). A total of 226 individuals that were

25 either CU or had MCI were included in these analyses. Of these dementia-free participants, 107

26 individuals eventually met the clinical criteria for a diagnosis of AD (mean follow-up, 3.8 years;

27 range, 0.5-16.5 years). Cox proportional hazards models revealed that individuals with plasma

28 IGFBP2 values greater than the 75th percentile exhibited a faster rate of conversion to AD, than

individuals with plasma IGFBP2 values less than the 25th percentile (hazard ratio (HR) 1.616, 95% confidence interval (CI) 1.074-2.430, $P = 0.021$, Fig. 6).

In the secondary analysis, baseline IGFBP2 plasma levels were kept as continuous, and 439 ADNI-1 dementia-free participants with plasma IGFBP2 measurements were included. Of these individuals, 214 were eventually diagnosed with AD (mean follow-up, 3.6 years; range, 0.5-16.5 years). Similar to the first model, elevated plasma IGFBP2 was associated with a greater rate of conversion to AD (HR 1.857, 95% CI 1.054-3.270, $P = 0.032$).

QFP cohort

Despite reductions in IGFBP2 mRNA, protein levels do not differ in the frontal cortex of AD brains

IGFBP2 gene expression was assessed by DNA microarray in the QFP cohort, and demonstrated to be significantly reduced in the frontal cortex of autopsy-confirmed AD brains ($n = 55$), compared to elderly controls ($n = 31$) ($P = 0.049$, Fig. 7A). However, as demonstrated through ELISA, IGFBP2 protein levels did not differ in the frontal cortex of AD cases ($n = 53$) after controlling for total protein levels, relative to controls ($n = 25$, $P = 0.462$, Fig. 7B).

Discussion

Our results suggest that nascent AD pathology induces a marked upregulation in IGFBP2, in asymptomatic individuals. CSF and plasma IGFBP2 behave as valuable biomarkers for identifying pre-clinical CSF Aβ(+)/t-tau(+) individuals, and those with a greater risk of AD conversion.

It has been well established that impaired insulin-IGF signalling plays a critical role in AD.[8-10] Furthermore, insulin and IGF proteins are highly expressed in the hippocampus.[8] Therefore, it is possible that impairments in insulin-IGF signaling may account for the selective vulnerability of the hippocampal formation to nascent AD pathology. Hence, targeting the insulin-IGF system may offer a promising solution to delay, slow down and/or prevent AD, either alone or in combination therapies. However, to develop these therapies, unraveling the molecular intricacies of the insulin-

17

1 IGF system is necessary. To this end, we investigated the role of the most abundant IGF-binding

2 protein in the CSF, IGFBP2,[28,29] during the earliest possible asymptomatic stage of AD, in "at-

3 risk", parental history-positive PREVENT-AD participants.

4 We observed a positive relationship between IGFBP2 and CSF $A\beta_{42}$ (Fig. 2A), which is consistent

5 with the proposed IGF-mediated clearance of $A\beta$.[12,13] This notion is in agreement with the finding

6 that current $A\beta$-lowering therapies induce an increase in CSF $A\beta_{42}$ in participants with MCI or

7 mild AD.[55] Furthermore, our data suggest IGFBP2 may be upregulated as a result of early neuronal

8 loss in the asymptomatic stage of the disease (Fig. 2C); which is consistent with the extensive

9 literature regarding the upregulation of IGFs and IGFBPs following several rodent models of brain

10 damage and recovery.[56-63] Furthermore, the administration of des-IGF-I, an analogue of IGF-1

11 with a low affinity for IGFBPs, failed to attenuate neuronal cell death in mice with experimental

12 hypoxic ischemic injuries.[64] However, the administration of IGFBP-compatible IGF-I

13 significantly reduced the observed neuronal loss.[64]

14 Our findings also suggest that IGFBP2 may be modulated by early CSF p_{181}-tau production (Fig.

15 2B) and early deposition in asymptomatic individuals. PET imaging analyses revealed that

16 IGFBP2 is positively associated (at a trend-level) with significant tau deposition in the entorhinal

17 cortex (Fig. 2E) and lingual gyrus (Supplementary Fig. 1), features that are typically associated

18 with early Braak Stages 2-3.[65] These findings are certainly consistent with the fact that insulin and

19 IGFs normally inhibit glycogen synthase kinase-3 (GSK3) activity and phospho-tau production in

20 human neurons, through the phosphoinositide 3-kinase-protein kinase B (PI3K-AKT) signaling

21 pathway.[14,15] For instance, the pharmacological inhibition of GSK3 has been linked to increases in

22 IGF-I in the rodent brain,[66] whereas conditional transgenic mice overexpressing GSK3 in the

23 cortex and hippocampus display increased tau phosphorylation in AD relevant epitopes,[67]

24 degeneration of the dentate gyrus[68] and spatial memory impairments.[69] Finally, mice

25 overexpressing IGFBP2 display an increase in AKT activity, a GSK3 inhibitor, in the brain.[70]

26 Thus, it is tempting to postulate that IGF regulation of GSK3 activity in turn modulates IGFBP2

27 production via a phospho-tau mediated process that ensures some form of local autoregulation

28 and/or resilience.

29 Given the prominent loss of synapses in AD, we examined the relationship between IGFBP2 and

30 synaptic proteins in the CSF, namely SNAP25 (Fig. 2F), SYT1 (Fig. 2G), GAP43 (Fig. 2H) and

1   NRGN (Fig. 2I).[40-45] The present study's results suggest that synaptic dysfunction and loss may

2   trigger an increase in IGFBP2 synthesis and secretion. This finding is in agreement with the

3   upregulation and regenerative abilities of IGFs to grow axons during the development of the CNS

4   and regrow axons during repair following injury to the CNS and/or PNS.[21,71-76]

5   Considering the relationship between CSF synaptic markers and CSF IGFBP2, we were interested

6   in examining the relationship between changes in cognition and baseline CSF IGFBP2 in

7   PREVENT-AD. We have demonstrated that CSF IGFBP2 levels are associated with cognitive

8   decline in RBANS delayed memory and visuospatial abilities over a 5-8-year period, in a subset

9   of PREVENT-AD participants (Fig. 3). This finding is consistent with a report that plasma levels

10   of IGFBP2 were negatively correlated with episodic memory performances in participants from

11   the ADNI cohort.[77] Thus, given the critical role of the hippocampus in the consolidation of

12   declarative memory and in spatial processing, our data provide compelling evidence that IGFBP2

13   plays a pivotal role in the integrity of the hippocampal formation, which displays elevated

14   expression levels of insulin, IGFs and their receptors – compared to other brain regions, such as

15   the frontal cortex.[8] Indeed, plasma IGFBP2 levels have been demonstrated to be negatively

16   correlated with hippocampal volumes in amyloid-negative individuals from the ADNI cohort.[77]

17   Consistent with this view, IGFBP2 has been demonstrated to be expressed by neurons and

18   astrocytes in the hippocampus during development and following CNS injury.[57-59,62,78,79]

19   Furthermore, the relationship between IGFBP2, delayed memory and hippocampal structure is

20   consistent with the finding that the administration of IGFBP2 has been shown to increase the

21   number of dendritic spines in the dentate gyrus of rodent models of post-traumatic stress disorder.[80]

22   In a similar fashion, in cell culture experiments, antibodies targeted against IGFBP2 have been

23   demonstrated to inhibit neurogenesis – a phenomenon that occurs in the dentate gyrus.[81] Moreover,

24   *IGFBP2* knockout mice exhibit deficits in long-term potentiation as well as impaired performances

25   on the Morris water maze, which heavily relies on the hippocampus.[79] Finally, the administration

26   of an IGFBP2-derived peptide has been demonstrated to rescue deficits in synaptic plasticity,

27   memory and learning in a mouse model of *SHANK3*-mediated post-synaptic deficits.[82] Overall,

28   these findings suggest that IGFBP2 in certain circumstances is linked to neuroprotection and

29   hippocampal-mediated cognitive abilities.

30   Indeed, it is important to take into consideration the early involvement of IGFBP2 in the

31   presymptomatic phase of AD, when presumably resilience is a major player in the brain response

19

to early neurodegeneration. For instance, several neuroprotective genes have been demonstrated to be upregulated by the (soluble) α-secretase cleaved fragment of amyloid precursor protein (sAPPα), amongst them, *IGFBP2* and *IGF2*.[83] Thus, it is possible that an increase in binding of IGFBP2 to IGFs may attenuate IGF degradation and/or promote the targeting of IGFs to their receptors, thus enhancing synaptic and terminal resilience in face of the emerging neurodegenerative process. This receptor targeting hypothesis is notably supported by evidence that transgenic mice overexpressing IGFBP2 lacking a proteoglycan-binding domain exhibit severe reductions in synaptic markers and hippocampal weight.[84] Finally, in a pilot study conducted on AD brains, temporal cortex IGFBP2 levels were negatively correlated with senile plaque levels – suggesting a role for IGFBP2 in neuroprotection and resilience.[9]

Given the negative relationship between IGFBP2 and cognitive abilities, we were prompted to examine whether baseline levels of CSF IGFBP2 were associated with anatomical changes in the brain. Interestingly, in asymptomatic PREVENT-AD participants, IGFBP2 was associated with atrophy in the left entorhinal cortex, at a trend-level (Fig. 4A). This is a critical finding, as the entorhinal cortex is the first region that is affected in AD.[65,85,86] Furthermore, IGFBP2 was associated with cortical thinning in several pre-specified temporal and parietal brain regions that are known to be affected early on in AD, such as the piriform cortex (Fig. 4B), inferior (Fig. 4C) and middle temporal gyri (Fig. 4D), and precuneus (Supplementary Fig. 2).[87,88] Overall, the structural neuroimaging results are in agreement with previous reports of IGFBP2 being associated with atrophy in AD-associated brain regions.[36,89,90]

Finally, in the PREVENT-AD cohort, changes in CSF IGFBP2 appear to be mostly specific to changes in the CNS, as we did not detect any significant peripheral vascular contributions or blood brain barrier dysfunction in these asymptomatic individuals (Supplementary Fig. 3).[54]

To independently validate our observations, we further analyzed data from a well-characterized cohort of CU individuals and individuals with MCI from ADNI-1 (Fig. 5A). Our results suggest that elevated CSF (Fig. 5B, Supplementary Fig. 4, Supplementary Fig. 5) and plasma IGFBP2 (Fig. 5C) may be valuable biomarkers of CSF Aβ(+)/t-tau(+) individuals and thus, facilitate screening for suitable patients for clinical trials.[50,51] This is not the first time that we identified a strong biphasic response as individuals progress from the CSF Aβ(+)/t-tau(-) stage to the CSF Aβ+/t-tau(+) stage (Supplementary Fig. 4, Supplementary Fig. 5). Certain inflammatory proteins

such as IL-8, IL-12 and IL-15 display the same initial reduction in the CSF Aβ(+)/t-tau(-) stage followed by marked increases in the CSF Aβ(+)/t-tau(+) stage.[91] These results support recent observations that immune activation may become apparent only after the onset of both amyloid and tau pathologies. Unexpectedly, these results also suggest that immune marker activity and IGFBP2 may diminish upon the earliest appearance of amyloid plaque pathology. However, as IGFBP2 regulates IGF signaling in neurons, one might speculate that an increase in binding of IGFBP2 to a limited amount of IGFs may block IGF-mediated suppression of tau phosphorylation, leading to increased levels of phospho-tau and ultimately, promoting tau deposition, neuronal damage and death.

Consistent with this working model and upon conducting survival analyses, we found that elevated circulating IGFBP2 levels were associated with a pronounced rate of conversion to AD in the ADNI cohort (Fig. 6). Overall, our results are consistent with the existing literature that plasma IGFBP2 has been associated with a greater risk of developing AD.[35,37,38] Finally, in contrast to the PREVENT-AD cohort, CSF IGFBP2 immunoassay measurements have been previously found to correlate with plasma IGFBP2 levels in the ADNI cohort – which incorporates individuals with a disrupted BBB.[77]

Finally, given the regional-specificity of the insulin-IGF system, we further examined IGFBP2 levels in the human brain.[8] IGFBP2 mRNA levels were reduced in the frontal cortex of autopsy-confirmed AD brains from the QFP cohort (Fig. 7A). However, cortical IGFBP2 protein levels did not differ between AD brains and elderly controls (Fig. 7B). Thus, our results provide further evidence that support the (hippocampal) regional specificity of the insulin-IGF system, potentially including the IGFBP2 protein.[8] However, due to the scarcity of medial temporal lobe tissues, we were unable to confirm the regional specificity of the IGFBP2 protein in the QFP cohort. Nevertheless, our results differ from those of a pilot study, that found IGFBP2 was decreased in the temporal cortex of AD brains.[9] It is possible our results differ since we measured cytoplasmic and extracellular IGFBP2, whilst the pilot study measured membrane-bound IGFBP2.[9] Finally, although IGFBP2 has been demonstrated to contain a nuclear localization signal and regulate the expression of several genes such as vascular endothelial growth factor, we were unable to differentiate between IGF-dependent and IGF-independent IGFBP2.[92]

Overall, our data suggest that IGFBP2 may play a critical role in neuroprotection during the asymptomatic stage of AD. However, as amyloid and tau pathology accumulate, the involvement of IGFBP2 appears to notably change. At that stage, elevated concentrations of IGFPB2 are associated with an accelerated rate of MCI to AD conversion in the ADNI cohort, and with subtle declines in delayed memory and visuospatial abilities in asymptomatic PREVENT-AD participants.

In the larger context of the insulin-IGF system, it will be exciting to follow the results of ongoing phase 3 clinical trials involving the administration of semaglutide (Ozempic), a glucagon-like peptide-1 receptor agonist that is clinically approved for the treatment of type 2 diabetes.[93] Considering the role of semaglutide in stimulating insulin secretion and signalling,[93] exploring therapeutic strategies that enhance IGF signalling in the brain,[94] perhaps through IGFBP2, may also warrant further investigation in presymptomatic AD. At the moment, we favor the hypothesis that an anti-IGFBP2 therapy may be effective in amyloid positive individuals whose tau deposition is minimal. As tau pathology emerges, it may prove difficult to change this complex metabolic process as IGFBP2 activity appears less protective and more reactive, similar to many other immune regulators.

Data availability

Data pertaining to the PREVENT-AD cohort can be downloaded from data release 6.0 at https://openpreventad.loris.ca/. CSF, plasma, genetic and clinical data from the ADNI-1 cohort were downloaded from the ADNI website (http://adni.loni.usc.edu/). Data collected from the QFP cohort are not publicly available, however the data are available from the corresponding author upon reasonable request.

Acknowledgements

Funding

23

24

Competing interests

JP serves as a scientific advisor to the Alzheimer Society of France. HZ has served at scientific advisory boards and/or as a consultant for Abbvie, Acumen, Alector, Alzinova, ALZPath, Annexon, Apellis, Artery Therapeutics, AZTherapies, CogRx, Denali, Eisai, Nervgen, Novo Nordisk, Optoceutics, Passage Bio, Pinteon Therapeutics, Prothena, Red Abbey Labs, reMYND, Roche, Samumed, Siemens Healthineers, Triplet Therapeutics, and Wave, has given lectures in symposia sponsored by Cellectricon, Fujirebio, Alzecure, Biogen, and Roche, and is a co-founder of Brain Biomarker Solutions in Gothenburg AB (BBS), which is a part of the GU Ventures Incubator Program (outside submitted work). KB has served as a consultant and at advisory boards for Acumen, ALZPath, BioArctic, Biogen, Eisai, Lilly, Moleac Pte. Ltd, Novartis, Ono Pharma, Prothena, Roche Diagnostics, and Siemens Healthineers; has served at data monitoring committees for Julius Clinical and Novartis; has given lectures, produced educational materials and participated in educational programs for AC Immune, Biogen, Celdara Medical, Eisai and Roche Diagnostics; and is a co-founder of Brain Biomarker Solutions in Gothenburg AB (BBS), which is a part of the GU Ventures Incubator Program, outside the work presented in this paper.

Supplementary material

Supplementary material is available at *Brain* online.

References

1. GBD 2019 Dementia Forecasting Collaborators. Estimation of the global prevalence of dementia in 2019 and forecasted prevalence in 2050: an analysis for the Global Burden of Disease Study 2019. *Lancet Public Health*. 2022;7(2):e105-e125. doi:10.1016/S2468-2667(21)00249-8

2. Nandi A, Counts N, Chen S, *et al*. Global and regional projections of the economic burden of Alzheimer's disease and related dementias from 2019 to 2050: A value of statistical life approach. *EClinicalMedicine*. 2022;51:101580. doi:10.1016/j.eclinm.2022.101580

3. Alzheimer's Association. 2022 Alzheimer's disease facts and figures. *Alzheimers Dement*. 2022;18(4):700-789. doi:10.1002/alz.12638

4. Serrano-Pozo A, Frosch MP, Masliah E, Hyman BT. Neuropathological alterations in Alzheimer disease. *Cold Spring Harbor Perspect Med*. 2011;1(1):a006189. doi:10.1101/cshperspect.a006189

5. Jack CR Jr, Knopman DS, Jagust WJ, *et al*. Hypothetical model of dynamic biomarkers of the Alzheimer's pathological cascade. *Lancet Neurol*. 2010;9(1):119-128. doi:10.1016/S1474-4422(09)70299-6

6. Arvanitakis Z, Wilson RS, Bienias JL, Evans DA, Bennett DA. Diabetes mellitus and risk of Alzheimer disease and decline in cognitive function. *Arch Neurol*. 2004;61(5):661-666. doi:10.1001/archneur.61.5.661

7. Arnold SE, Arvanitakis Z, Macauley-Rambach SL, *et al*. Brain insulin resistance in type 2 diabetes and Alzheimer disease: concepts and conundrums. *Nat Rev Neurol*. 2018;14(3):168-181. doi:10.1038/nrneurol.2017.185

8. Steen E, Terry BM, J Rivera E, *et al*. Impaired insulin and insulin-like growth factor expression and signaling mechanisms in Alzheimer's disease–is this type 3 diabetes?. *J Alzheimers Dis*. 2005;7(1):63-80. doi:10.3233/jad-2005-7107

9. Moloney AM, Griffin RJ, Timmons S, O'Connor R, Ravid R, O'Neill C. Defects in IGF-1 receptor, insulin receptor and IRS-1/2 in Alzheimer's disease indicate possible resistance to IGF-1 and insulin signalling. *Neurobiol Aging*. 2010;31(2):224-243. doi:10.1016/j.neurobiolaging.2008.04.002

10. Talbot K, Wang HY, Kazi H, *et al*. Demonstrated brain insulin resistance in Alzheimer's disease patients is associated with IGF-1 resistance, IRS-1 dysregulation, and cognitive decline. *J Clin Invest*. 2012;122(4):1316-1338. doi:10.1172/JCI59903

11. Kar S, Poirier J, Guevara J, *et al*. Cellular distribution of insulin-like growth factor-II/mannose-6-phosphate receptor in normal human brain and its alteration in Alzheimer's

26

disease pathology. *Neurobiol Aging*. 2006;27(2):199-210. doi:10.1016/j.neurobiolaging.2005.03.005

12. Farris W, Mansourian S, Chang Y, *et al*. Insulin-degrading enzyme regulates the levels of insulin, amyloid β-protein, and the β-amyloid precursor protein intracellular domain in vivo. *Proc Natl Acad Sci U S A*. 2003;100(7):4162-4167. doi:10.1073/pnas.0230450100

13. Carro E, Trejo JL, Gomez-Isla T, LeRoith D, Torres-Aleman I. Serum insulin-like growth factor I regulates brain amyloid-β levels. *Nat Med*. 2002;8(12):1390-1397. doi:10.1038/nm1202-793

14. Hong M, Lee VM. Insulin and insulin-like growth factor-1 regulate tau phosphorylation in cultured human neurons. *J Biol Chem*. 1997;272(31):19547-19553. doi:10.1074/jbc.272.31.19547

15. Schubert M, Brazil DP, Burks DJ, *et al*. Insulin receptor substrate-2 deficiency impairs brain growth and promotes tau phosphorylation. *J Neurosci*. 2003;23(18):7084-7092. doi:10.1523/JNEUROSCI.23-18-07084.2003

16. De Felice FG, Vieira MN, Bomfim TR, *et al*. Protection of synapses against Alzheimer's-linked toxins: insulin signaling prevents the pathogenic binding of Aβ oligomers. *Proc Natl Acad Sci U S A*. 2009;106(6):1971-1976. doi:10.1073/pnas.0809158106

17. Doré S, Kar S, Quirion R. Insulin-like growth factor I protects and rescues hippocampal neurons against beta-amyloid- and human amylin-induced toxicity. *Proc Natl Acad Sci U S A*. 1997;94(9):4772-4777. doi:10.1073/pnas.94.9.4772

18. Willette AA, Bendlin BB, Starks EJ, *et al*. Association of Insulin Resistance With Cerebral Glucose Uptake in Late Middle-Aged Adults at Risk for Alzheimer Disease. *JAMA Neurol*. 2015;72(9):1013-1020. doi:10.1001/jamaneurol.2015.0613

19. Reger MA, Watson GS, Green PS, *et al*. Intranasal insulin improves cognition and modulates beta-amyloid in early AD. *Neurology*. 2008;70(6):440-448. doi:10.1212/01.WNL.0000265401.62434.36

20. Craft S, Baker LD, Montine TJ, *et al*. Intranasal insulin therapy for Alzheimer disease and amnestic mild cognitive impairment: a pilot clinical trial. *Arch Neurol*. 2012;69(1):29-38. doi:10.1001/archneurol.2011.233

21. O'Kusky JR, Ye P, D'Ercole AJ. Insulin-like growth factor-I promotes neurogenesis and synaptogenesis in the hippocampal dentate gyrus during postnatal development. *J Neurosci*. 2000;20(22):8435-8442. doi:10.1523/JNEUROSCI.20-22-08435.2000

22. Russo VC, Gluckman PD, Feldman EL, Werther GA. The insulin-like growth factor system and its pleiotropic functions in brain. *Endocr Rev*. 2005;26(7):916-43. doi:10.1210/er.2004-0024

23. Allard JB, Duan C. IGF-binding proteins: why do they exist and why are there so many?. *Front Endocrinol (Lausanne)*. 2018;9:117. doi:10.3389/fendo.2018.00117

24. Hwa V, Oh Y, Rosenfeld RG. The insulin-like growth factor-binding protein (IGFBP) superfamily. *Endocr Rev*. 1999;20(6):761-787. doi:10.1210/edrv.20.6.0382

25. Russo VC, Bach LA, Fosang AJ, Baker NL, Werther GA. Insulin-like growth factor binding protein-2 binds to cell surface proteoglycans in the rat brain olfactory bulb. *Endocrinology*. 1997;138(11):4858-4867. doi:10.1210/endo.138.11.5472

26. Schütt BS, Langkamp M, Rauschnabel U, Ranke MB, Elmlinger MW. Integrin-mediated action of insulin-like growth factor binding protein-2 in tumor cells. *J Mol Endocrinol*. 2004;32(3):859-868. doi:10.1677/jme.0.0320859

27. Russo VC, Rekaris G, Baker NL, Bach LA, Werther GA. Basic fibroblast growth factor induces proteolysis of secreted and cell membrane-associated insulin-like growth factor binding protein-2 in human neuroblastoma cells. *Endocrinology*. 1999;140(7):3082-3090. doi:10.1210/endo.140.7.6771

28. Roghani M, Lassarre C, Zapf J, Povoa G, Binoux M. Two insulin-like growth factor (IGF)-binding proteins are responsible for the selective affinity for IGF-II of cerebrospinal fluid binding proteins. *J Clin Endocrinol Metab*. 1991;73(3):658-666. doi:10.1210/jcem-73-3-658

29. Ocrant I, Fay CT, Parmelee JT. Characterization of insulin-like growth factor binding proteins produced in the rat central nervous system. *Endocrinology*. 1990;127(3):1260-1267. doi:10.1210/endo-127-3-1260

30. Tham A, Nordberg A, Grissom FE, Carlsson-Skwirut C, Viitanen M, Sara VR. Insulin-like growth factors and insulin-like growth factor binding proteins in cerebrospinal fluid and

serum of patients with dementia of the Alzheimer type. *J Neural Transm Park Dis Dement Sect*.1993;5(3):165-176. doi:10.1007/BF02257671

31. Salehi Z, Mashayekhi F, Naji M. Insulin like growth factor-1 and insulin like growth factor binding proteins in the cerebrospinal fluid and serum from patients with Alzheimer's disease. *Biofactors*. 2008;33(2):99-106. doi:10.1002/biof.5520330202

32. Hertze J, Nägga K, Minthon L, Hansson O. Changes in cerebrospinal fluid and blood plasma levels of IGF-II and its binding proteins in Alzheimer's disease: an observational study. *BMC Neurol*. 2014;14:64. doi:10.1186/1471-2377-14-64

33. Åberg D, Johansson P, Isgaard J, *et al*. Increased cerebrospinal fluid level of insulin-like growth factor-II in male patients with Alzheimer's disease. *J Alzheimers Dis*. 2015;48(3):637-646. doi:10.3233/JAD-150351

34. O'Bryant SE, Xiao G, Barber R, *et al*. A serum protein-based algorithm for the detection of Alzheimer disease. *Arch Neurol*. 2010;67(9):1077-1081. doi:10.1001/archneurol.2010.215

35. Doecke JD, Laws SM, Faux NG, *et al*. Blood-based protein biomarkers for diagnosis of Alzheimer disease. *Arch Neurol*. 2012;69(10):1318-1325. doi:10.1001/archneurol.2012.1282

36. Bonham LW, Geier EG, Steele NZ, *et al*. Insulin-like growth factor binding protein 2 is associated with biomarkers of Alzheimer's disease pathology and shows differential expression in transgenic mice. *Front Neurosci*. 2018;12:476. doi:10.3389/fnins.2018.00476

37. McGrath ER, Himali JJ, Levy D, *et al*. Circulating IGFBP-2: a novel biomarker for incident dementia. *Ann Clin Transl Neurol*. 2019;6(9):1659-1670. doi:10.1002/acn3.50854

38. Rocha de Paula M, Gómez Ravetti M, Berretta R, Moscato P. Differences in abundances of cell-signalling proteins in blood reveal novel biomarkers for early detection of clinical Alzheimer's disease. *PLoS One*. 2011;6(3):e17481. doi:10.1371/journal.pone.0017481

39. Tremblay-Mercier J, Madjar C, Das S, *et al*. Open science datasets from PREVENT-AD, a longitudinal cohort of pre-symptomatic Alzheimer's disease. *Neuroimage Clin*. 2021;31:102733. doi:10.1016/j.nicl.2021.102733

40. Brinkmalm A, Brinkmalm G, Honer WG, *et al*. SNAP-25 is a promising novel cerebrospinal fluid biomarker for synapse degeneration in Alzheimer's disease. *Mol Neurodegener*. 2014;9:53. doi:10.1186/1750-1326-9-53

41. Öhrfelt A, Brinkmalm A, Dumurgier J, *et al*. The pre-synaptic vesicle protein synaptotagmin is a novel biomarker for Alzheimer's disease. *Alzheimers Res Ther*. 2016;8(1):41. doi:10.1186/s13195-016-0208-8

42. Tible M, Sandelius Å, Höglund K, *et al*. Dissection of synaptic pathways through the CSF biomarkers for predicting Alzheimer disease. *Neurology*. 2020;95(8):e953-e961. doi:10.1212/WNL.0000000000010131

43. Xu C, Sellgren CM, Fatouros-Bergman H, *et al*. CSF levels of synaptosomal-associated protein 25 and synaptotagmin-1 in first-episode psychosis subjects. *IBRO Rep*. 2020;8:136-142. doi:10.1016/j.ibror.2020.04.001

44. Sandelius Å, Portelius E, Källén Å, *et al*. Elevated CSF GAP-43 is Alzheimer's disease specific and associated with tau and amyloid pathology. *Alzheimers Dement*. 2019;15(1):55-64. doi:10.1016/j.jalz.2018.08.006

45. Portelius E, Olsson B, Höglund K, *et al*. Cerebrospinal fluid neurogranin concentration in neurodegeneration: relation to clinical phenotypes and neuropathology. *Acta Neuropathol*. 2018;136(3):363-376. doi:10.1007/s00401-018-1851-x

46. McSweeney M, Binette AP, Meyer PF, *et al*. Intermediate flortaucipir uptake is associated with Aβ-PET and CSF tau in asymptomatic adults. *Neurology*. 2020;94(11):e1190-1200. doi:10.1212/WNL.0000000000008905

47. Zijdenbos AP, Forghani R, Evans AC. Automatic "pipeline" analysis of 3-D MRI data for clinical trials: application to multiple sclerosis. *IEEE Trans Med Imaging*. 2002;21(10):1280–1291. doi:10.1109/TMI.2002.806283

48. Aubert-Broche B, Fonov VS, García-Lorenzo D, *et al*. A new method for structural volume analysis of longitudinal brain MRI data and its application in studying the growth trajectories of anatomical brain structures in childhood. *Neuroimage*. 2013;82:393-402. doi:10.1016/j.neuroimage.2013.05.065

49. Randolph C, Tierney MC, Mohr E, Chase TN. The Repeatable Battery for the Assessment of Neuropsychological Status (RBANS): preliminary clinical validity. *J Clin Exp Neuropsychol*. 1998;20(3):310-319. doi:10.1076/jcen.20.3.310.823

50. Jack CR Jr, Bennett DA, Blennow K, *et al*. NIA-AA research framework: toward a biological definition of Alzheimer's disease. *Alzheimers Dement*. 2018;14(4):535-562. doi:10.1016/j.jalz.2018.02.018

51. Shaw LM, Vanderstichele H, Knapik-Czajka M, *et al*. Cerebrospinal fluid biomarker signature in Alzheimer's disease neuroimaging initiative subjects. *Ann Neurol*. 2009;65(4):403-413. doi:10.1002/ana.21610

52. Scriver CR. Human genetics: lessons from Quebec populations. *Annu Rev Genomics Hum Genet*. 2001;2:69-101. doi:10.1146/annurev.genom.2.1.69

53. McKhann G, Drachman D, Folstein M, Katzman R, Price D, Stadlan EM. Clinical diagnosis of Alzheimer's disease: Report of the NINCDS-ADRDA Work Group* under the auspices of Department of Health and Human Services Task Force on Alzheimer's Disease. *Neurology*. 1984;34(7):939-944. doi:10.1212/wnl.34.7.939

54. Picard C, Nilsson N, Labonté A, *et al*. Apolipoprotein B is a novel marker for early tau pathology in Alzheimer's disease. *Alzheimers Dement*. 2022;18(5):875-887. doi:10.1002/alz.12442

55. van Dyck CH, Swanson CJ, Aisen P, *et al*. Lecanemab in Early Alzheimer's Disease. *N Engl J Med*. 2023;388(1):9-21. doi:10.1056/NEJMoa2212948

56. Gluckman P, Klempt N, Guan J, *et al*. A role for IGF-1 in the rescue of CNS neurons following hypoxic-ischemic injury. *Biochem Biophys Res Commun*. 1992;182(2):593-599. doi:10.1016/0006-291x(92)91774-k

57. Klempt ND, Klempt M, Gunn AJ, Singh K, Gluckman PD. Expression of insulin-like growth factor-binding protein 2 (IGF-BP 2) following transient hypoxia-ischemia in the infant rat brain. *Brain Res Mol Brain Res*. 1992;15(1-2):55-61. doi:10.1016/0169-328x(92)90151-z

58. Beilharz EJ, Russo VC, Butler G, *et al*. Co-ordinated and cellular specific induction of the components of the IGF/IGFBP axis in the rat brain following hypoxic–ischemic injury. *Brain Res Mol Brain Res*. 1998;59(2):119-134. doi:10.1016/s0169-328x(98)00122-3

59. Sandberg Nordqvist AC, Von Holst H, Holmin S, Sara VR, Bellander BM, Schalling M. Increase of insulin-like growth factor (IGF)-1, IGF binding protein-2 and− 4 mRNAs following cerebral contusion. *Brain Res Mol Brain Res*. 1996;38(2):285-293. doi:10.1016/0169-328x(95)00346-t

60. Walter HJ, Berry M, Hill DJ, Logan A. Spatial and temporal changes in the insulin-like growth factor (IGF) axis indicate autocrine/paracrine actions of IGF-I within wounds of the rat brain. *Endocrinology*. 1997;138(7):3024-3034. doi:10.1210/endo.138.7.5284

61. Fletcher L, Isgor E, Sprague S, *et al*. Spatial distribution of insulin-like growth factor binding protein-2 following hypoxic-ischemic injury. *BMC Neurosci*. 2013;14:158. doi:10.1186/1471-2202-14-158

62. Breese CR, D'Costa A, Rollins YD, *et al*. Expression of insulin-like growth factor-1 (IGF-1) and IGF-binding protein 2 (IGF-BP2) in the hippocampus following cytotoxic lesion of the dentate gyrus. *J Comp Neurol*. 1996;369(3):388-404. doi:10.1002/(SICI)1096-9861(19960603)369:3<388::AID-CNE5>3.0.CO;2-1

63. Kar S, Baccichet A, Quirion R, Poirier J. Entorhinal cortex lesion induces differential responses in [125I]insulin-like growth factor I, [125I]insulin-like growth factor II and [125I]insulin receptor binding sites in the rat hippocampal formation. *Neuroscience*. 1993;55(1):69-80. doi:10.1016/0306-4522(93)90455-o

64. Guan J, Williams CE, Skinner SJ, Mallard EC, Gluckman PD. The effects of insulin-like growth factor (IGF)-1, IGF-2, and des-IGF-1 on neuronal loss after hypoxic-ischemic brain injury in adult rats: evidence for a role for IGF binding proteins. *Endocrinology*. 1996;137(3):893-898. doi:10.1210/endo.137.3.8603600

65. Braak H, Braak E. Staging of Alzheimer's disease-related neurofibrillary changes. *Neurobiol Aging*. 1995;16(3):271-284. doi:10.1016/0197-4580(95)00021-6

66. Bolós M, Fernandez S, Torres-Aleman I. Oral administration of a GSK3 inhibitor increases brain insulin-like growth factor I levels. *J Biol Chem*. 2010;285(23):17693-17700. doi:10.1074/jbc.M109.096594

67. Lucas JJ, Hernández F, Gómez-Ramos P, Morán MA, Hen R, Avila J. Decreased nuclear beta-catenin, tau hyperphosphorylation and neurodegeneration in GSK-3beta conditional transgenic mice. *EMBO J*. 2001;20(1-2):27-39. doi:10.1093/emboj/20.1.27

68. Engel T, Lucas JJ, Gómez-Ramos P, Moran MA, Avila J, Hernández F. Cooexpression of FTDP-17 tau and GSK-3beta in transgenic mice induce tau polymerization and neurodegeneration. *Neurobiol Aging*. 2006;27(9):1258-1268. doi:10.1016/j.neurobiolaging.2005.06.010

69. Hernández F, Borrell J, Guaza C, Avila J, Lucas JJ. Spatial learning deficit in transgenic mice that conditionally over-express GSK-3beta in the brain but do not form tau filaments. *J Neurochem*. 2002;83(6):1529-1533. doi:10.1046/j.1471-4159.2002.01269.x

70. Hoeflich A, Reyer A, Ohde D, *et al*. Dissociation of somatic growth, time of sexual maturity, and life expectancy by overexpression of an RGD-deficient IGFBP-2 variant in female transgenic mice. *Aging Cell*. 2016;15(1):111-117. doi:10.1111/acel.12413

71. Kanje M, Skottner A, Sjöberg J, Lundborg G. Insulin-like growth factor I (IGF-I) stimulates regeneration of the rat sciatic nerve. *Brain Res*. 1989;486(2):396-398. doi:10.1016/0006-8993(89)90531-3

72. Near SL, Whalen LR, Miller JA, Ishii DN. Insulin-like growth factor II stimulates motor nerve regeneration. *Proc Natl Acad Sci U S A*. 1992;89(24):11716-11720. doi:10.1073/pnas.89.24.11716

73. Guthrie KM, Nguyen T, Gall CM. Insulin-like growth factor-1 mRNA is increased in deafferented hippocampus: spatiotemporal correspondence of a trophic event with axon sprouting. *J Comp Neurol*. 1995;352(1):147-160. doi:10.1002/cne.903520111

74. Duan X, Qiao M, Bei F, Kim IJ, He Z, Sanes JR. Subtype-specific regeneration of retinal ganglion cells following axotomy: effects of osteopontin and mTOR signaling. *Neuron*. 2015;85(6):1244-1256. doi:10.1016/j.neuron.2015.02.017

33

75. Anderson MA, O'Shea TM, Burda JE, *et al.* Required growth facilitators propel axon regeneration across complete spinal cord injury. *Nature*. 2018;561(7723):396-400. doi:10.1038/s41586-018-0467-6

76. Liu Y, Wang X, Li W, *et al.* A Sensitized IGF1 Treatment Restores Corticospinal Axon-Dependent Functions. *Neuron*. 2017;95(4):817-833.e4. doi:10.1016/j.neuron.2017.07.037

77. Lane EM, Hohman TJ, Jefferson AL, Alzheimer's Disease Neuroimaging Initiative. Insulin-like growth factor binding protein-2 interactions with Alzheimer's disease biomarkers. *Brain Imaging Behav*. 2017;11(6):1779-1786. doi:10.1007/s11682-016-9636-0

78. Lee WH, Michels KM, Bondy CA. Localization of insulin-like growth factor binding protein-2 messenger RNA during postnatal brain development: correlation with insulin-like growth factors I and II. *Neuroscience*. 1993;53(1):251-265. doi:10.1016/0306-4522(93)90303-w

79. Khan S, Lu X, Huang Q, *et al.* IGFBP2 plays an essential role in cognitive development during early life. *Adv Sci (Weinh)*. 2019;6(23):1901152. doi:10.1002/advs.201901152

80. Burgdorf J, Colechio EM, Ghoreishi-Haack N, *et al.* IGFBP2 produces rapid-acting and long-lasting effects in rat models of posttraumatic stress disorder via a novel mechanism associated with structural plasticity. *Int J Neuropsychopharmacol*. 2017;20(6):476-484. doi:10.1093/ijnp/pyx007

81. Brooker GJ, Kalloniatis M, Russo VC, Murphy M, Werther GA, Bartlett PF. Endogenous IGF-1 regulates the neuronal differentiation of adult stem cells. *J Neurosci Res*. 2000;59(3):332-341. doi:10.1002/(sici)1097-4547(20000201)59:3<332::aid-jnr6>3.0.co;2-2

82. Burgdorf JS, Yoon S, Dos Santos M, Lammert CR, Moskal JR, Penzes P. An IGFBP2-derived peptide promotes neuroplasticity and rescues deficits in a mouse model of Phelan-McDermid syndrome. *Mol Psychiatry*. 2023;28(3):1101-1111. doi:10.1038/s41380-022-01904-0

83. Stein TD, Anders NJ, DeCarli C, Chan SL, Mattson MP, Johnson JA. Neutralization of transthyretin reverses the neuroprotective effects of secreted amyloid precursor protein

(APP) in APPSW mice resulting in tau phosphorylation and loss of hippocampal neurons: support for the amyloid hypothesis. *J Neurosci*. 2004;24(35):7707-7717. doi:10.1523/JNEUROSCI.2211-04.2004

84. Schindler N, Mayer J, Saenger S, *et al*. Phenotype analysis of male transgenic mice overexpressing mutant IGFBP-2 lacking the Cardin-Weintraub sequence motif: Reduced expression of synaptic markers and myelin basic protein in the brain and a lower degree of anxiety-like behaviour. *Growth Horm IGF Res*. 2017;33:1-8. doi:10.1016/j.ghir.2016.11.003

85. Gómez-Isla T, Price JL, McKeel DW Jr, Morris JC, Growdon JH, Hyman BT. Profound loss of layer II entorhinal cortex neurons occurs in very mild Alzheimer's disease. *J Neurosci*. 1996;16(14):4491-4500. doi:10.1523/JNEUROSCI.16-14-04491.1996

86. Dickerson BC, Goncharova I, Sullivan MP, *et al*. MRI-derived entorhinal and hippocampal atrophy in incipient and very mild Alzheimer's disease. *Neurobiol Aging*. 2001;22(5):747-754. doi:10.1016/s0197-4580(01)00271-8

87. Dickerson BC, Bakkour A, Salat DH, *et al*. The cortical signature of Alzheimer's disease: regionally specific cortical thinning relates to symptom severity in very mild to mild AD dementia and is detectable in asymptomatic amyloid-positive individuals. *Cereb Cortex*. 2009;19(3):497-510. doi:10.1093/cercor/bhn113

88. Schwarz CG, Gunter JL, Wiste HJ, *et al*. A large-scale comparison of cortical thickness and volume methods for measuring Alzheimer's disease severity. *Neuroimage Clin*. 2016;11:802-812. doi:10.1016/j.nicl.2016.05.017

89. Toledo JB, Da X, Bhatt P, *et al*. Relationship between plasma analytes and SPARE-AD defined brain atrophy patterns in ADNI. *PLoS One*. 2013;8(2):e55531. doi:10.1371/journal.pone.0055531

90. McLimans KE, Webb JL, Anantharam V, Kanthasamy A, Willette AA, Alzheimer's Disease Neuroimaging Initiative. Peripheral versus Central Index of Metabolic Dysfunction and Associations with Clinical and Pathological Outcomes in Alzheimer's Disease. *J Alzheimers Dis*. 2017;60(4):1313-1324. doi:10.3233/JAD-170263

91. Meyer PF, Savard M, Poirier J, *et al*. Bi-directional Association of Cerebrospinal Fluid Immune Markers with Stage of Alzheimer's Disease Pathogenesis. *J Alzheimers Dis*. 2018;63(2):577-590. doi:10.3233/JAD-170887

92. Azar WJ, Zivkovic S, Werther GA, Russo VC. IGFBP-2 nuclear translocation is mediated by a functional NLS sequence and is essential for its pro-tumorigenic actions in cancer cells. *Oncogene*. 2014;33(5):578-588. doi:10.1038/onc.2012.630

93. Mahapatra MK, Karuppasamy M, Sahoo BM. Therapeutic Potential of Semaglutide, a Newer GLP-1 Receptor Agonist, in Abating Obesity, Non-Alcoholic Steatohepatitis and Neurodegenerative diseases: A Narrative Review. *Pharm Res*. 2022;39(6):1233-1248. doi:10.1007/s11095-022-03302-1

94. Doré S, Kar S, Quirion R. Rediscovering an old friend, IGF-I: potential use in the treatment of neurodegenerative diseases. *Trends Neurosci*. 1997;20(8):326-331. doi:10.1016/s0166-2236(96)01036-3

Figure legends

Figure 1 CSF IGFBP2 levels progressively increase over 5 years in asymptomatic PREVENT-AD participants. IGFBP2 was measured in the CSF of a subset of PREVENT-AD participants ($n = 27$) at baseline and at follow-up visits, using the Olink Proximity Extension Assay. Linear mixed models accounting for participant-specific trajectories demonstrate CSF IGFBP2 levels increase in a subset of at-risk individuals that have been followed for 5 years. β and *P* values are located in the top left corner. PREVENT-AD, PRe-symptomatic EVAluation of Experimental or Novel Treatments for Alzheimer's Disease; CSF, cerebrospinal fluid; IGFBP2, insulin-like growth factor binding protein-2; NPX, Normalized Protein eXpression.

1 **Figure 2 CSF IGFBP2 is associated with CSF and PET AD biomarkers in the asymptomatic**

2 **PREVENT-AD cohort.** CSF IGFBP2 levels were measured using the Olink Proximity Extension

3 Assay (n = 109). (**A**) CSF AD biomarkers Aβ_{42}, (**B**) p$_{181}$-tau and (**C**) t-tau were measured using

4 validated Innotest ELISA kits, following the standardized protocols established by the

5 BIOMARKAPD consortium (n = 101). (**D**) Global cortical amyloid SUVR was measured using

6 ^{18}F-NAV4694 (n = 46). (**E**) Tau deposition in the entorhinal cortex was measured with flortaucipir

7 (n = 49). The synaptic markers (**F**) SNAP-25 (n = 106), (**G**) SYT-1 (n = 106), (**H**) GAP43 (n =

8 46) and (**I**) NRGN (n = 46) were quantified using immunoprecipitation followed by mass

9 spectrometry. Significant or trend-level linear regressions are represented with a blue confidence

10 region of the fitted line. R^2 and P values are located in the top left corners of each panel. Analyses

11 were adjusted for age, sex and *APOE* ε4 carrier status. PREVENT-AD, PRe-symptomatic

12 EValuation of Experimental or Novel Treatments for Alzheimer's Disease; CSF, cerebrospinal

13 fluid; IGFBP2, insulin-like growth factor binding protein-2; NPX, Normalized Protein eXpression;

14 AD, Alzheimer's disease; Aβ_{42}, amyloid-beta 42; p$_{181}$-tau, phosphorylated tau at residue 181; t-

15 tau, total tau; ELISA, enzyme-linked immunosorbent assay; BIOMARKAPD, Biomarker's for

16 Alzheimer's and Parkinson's disease; PET, positron emission tomography; SUVR, standardized

17 uptake value ratio; SNAP-25, synaptosomal-associated protein 23kDa; a.u., arbitrary units; SYT1,

18 synaptotagmin-1; GAP43, growth-associated protein 43; pg/mL, picogram per millilitre NRGN,

19 neurogranin; APOE, apolipoprotein E.

20

21 **Figure 3 CSF IGFBP2 is associated with longitudinal changes in delayed memory and**

22 **visuospatial abilities over 5-8 years in PREVENT-AD.** CSF IGFBP2 levels were measured

23 using the Olink Proximity Extension Assay (n = 109). Cognitive performance trajectory slopes

24 were computed for each cognitive domain of the RBANS (delayed memory, visuospatial abilities,

25 language, immediate memory and attention) in a subset of PREVENT-AD participants that were

26 followed for 5-8 years (n = 89). Significant linear regressions are represented with a confidence

27 region of the fitted line (blue for delayed memory and red for visuospatial abilities). R^2, β and P

28 values are located in the top right corner. Analyses were adjusted for age, sex, *APOE* ε4 carrier

29 status and years of education. PREVENT-AD, PRe-symptomatic EValuation of Experimental or

30 Novel Treatments for Alzheimer's Disease; CSF, cerebrospinal fluid; IGFBP2, insulin-like growth

1   factor binding protein-2; NPX, Normalized Protein eXpression; RBANS, Repeatable Battery for

2   the Assessment of Neuropsychological Status; APOE, apolipoprotein E.

3

4   **Figure 4 CSF IGFBP2 is associated with atrophy in AD-related brain regions in PREVENT-**

5   **AD.** CSF IGFBP2 levels were measured using the Olink Proximity Extension Assay ($n = 109$).

6   T1-weighted structural MRI scans were performed on a subset of PREVENT-AD participants (n

7   $= 104$). The imaging processing pipeline CIVET 1.1.12 was used to analyze neuroimaging data.

8   (**A**) Entorhinal cortex volumes were normalized by total intracranial volumes. Cortical thickness

9   measurements were acquired from AD-related brain regions, such as the (**B**) piriform cortex, (**C**)

10 inferior temporal gyrus and (**D**) middle temporal gyrus. Significant or trend-level linear regressions

11 are represented with a confidence region of the fitted line (blue for left hemisphere and red for

12 right hemisphere). R^2 and P values are located in the top right corner of each panel. Analyses were

13 adjusted for age, sex and *APOE* ε4 carrier status. PREVENT-AD, PRe-symptomatic EVAluation

14 of Experimental or Novel Treatments for Alzheimer's Disease; AD, Alzheimer's disease; CSF,

15 cerebrospinal fluid; IGFBP2, insulin-like growth factor binding protein-2; NPX, Normalized

16 Protein eXpression; ICV, intracranial volume; mm, millimetres; MRI, magnetic resonance

17 imaging; APOE, apolipoprotein E.

18

19 **Figure 5 CSF and plasma IGFBP2 is elevated in CSF Aβ(+)/t-tau(+) individuals from the**

20 **ADNI-1 cohort.** (**A**) Cognitively unaffected participants (red, $n = 92$) and participants with MCI

21 (blue, $n = 149$) from the ADNI-1 cohort were staged as CSF amyloid and/or CSF total tau positive

22 according to the recommended thresholds of 192 pg/mL and 93 pg/mL. Linear models, adjusted

23 for age, sex and *APOE* ε4 carrier status were used to examine mean differences in IGFBP2 protein

24 levels across stages. (**B**) CSF IGFBP2 was elevated at Stage 2 ($n = 77$) relative to Stage 0 ($n = 80$)

25 and Stage 1 ($n = 68$). Furthermore, CSF IGFBP2 was elevated in SNAP ($n = 8$) compared to Stage

26 0. (**C**) Plasma IGFBP2 was elevated at Stage 2 ($n = 84$) relative to Stage 0 ($n = 98$) and Stage 1 (n

27 $= 60$). However, plasma IGFBP2 did not significantly differ between SNAP ($n = 12$) and Stage 0.

28 The data are represented as mean ± SEM. *$P < 0.05$; **$P < 0.01$. ADNI, Alzheimer's disease

29 neuroimaging initiative; CSF, cerebrospinal fluid; IGFBP2, insulin-like growth factor binding

30 protein-2; NPX, Normalized Protein eXpression; Aβ, amyloid-beta; Aβ$_{42}$, amyloid-beta 42; t-tau,

1 total tau; pg/mL, picogram per millilitre; SNAP, suspected non-Alzheimer pathology; MCI, mild

2 cognitive impairment; ng/mL, nanogram per millilitre; log, logarithm base 10; APOE,

3 apolipoprotein E; SEM, standard error of the mean.

4

5 **Figure 6 Elevated plasma IGFBP2 is associated with a greater rate of conversion to AD in**

6 **individuals from the ADNI-1 cohort.** Cox proportional hazards models examined the association

7 between baseline plasma IGFBP2 levels and rate of conversion to AD. The first quartile (blue) and

8 fourth (red) values of plasma IGFBP2 were contrasted. Participants were followed from the

9 baseline visit to the time of diagnosis (of AD), or to the time the participant was last confirmed to

10 be free of AD (mean follow-up, 3.8 years; range, 0.5-16.5 years). Of the 226 individuals that were

11 followed longitudinally, 107 individuals progressed to AD. Individuals with plasma IGFBP2

12 values in the fourth quartile exhibited a greater rate of conversion to AD, compared to the first

13 quartile. HR and *P* values are located in the top right corner. Cox models were adjusted for age,

14 gender and *APOE* ε4 carrier status. ADNI, Alzheimer's disease neuroimaging initiative; IGFBP2,

15 insulin-like growth factor binding protein-2; NPX, Normalized Protein eXpression; AD,

16 Alzheimer's disease; HR, hazard ratio; APOE, apolipoprotein E.

17

18 **Figure 7 Frontal cortex IGFBP2 gene expression is reduced in autopsy-confirmed AD brains,**

19 **however protein levels do not differ from elderly controls.** (**A**) Microarray technology was used

20 to measure IGFBP2 mRNA levels in the frontal cortex of autopsy-confirmed AD brains ($n = 55$)

21 and elderly controls ($n = 31$) from the QFP cohort. (**B**) IGFBP2 protein levels in the frontal cortex

22 were measured in AD brains ($n = 53$) and control brains ($n = 25$) using a commercially available

23 ELISA kit. Analyses were adjusted for age, sex, *APOE* ε4 carrier status and post-mortem interval.

24 The data are represented as mean ± SEM. *$P < 0.05$. QFP, Quebec Founder Population; IGFBP2,

25 insulin-like growth factor binding protein-2; mRNA, messenger RNA; log_2, logarithm base 2;

26 CTL, control; AD, Alzheimer's disease; ELISA, enzyme-linked immunosorbent assay; SEM,

27 standard error of the mean; APOE, apolipoprotein E, SEM, standard error of the mean.
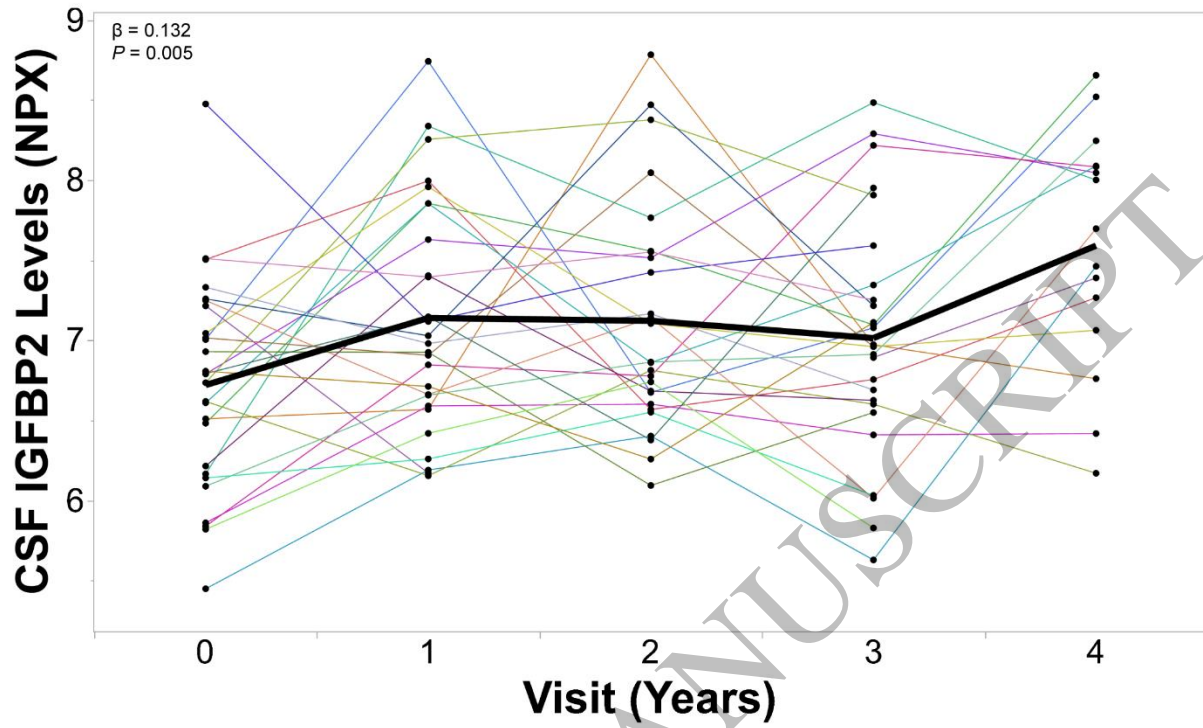
28

29
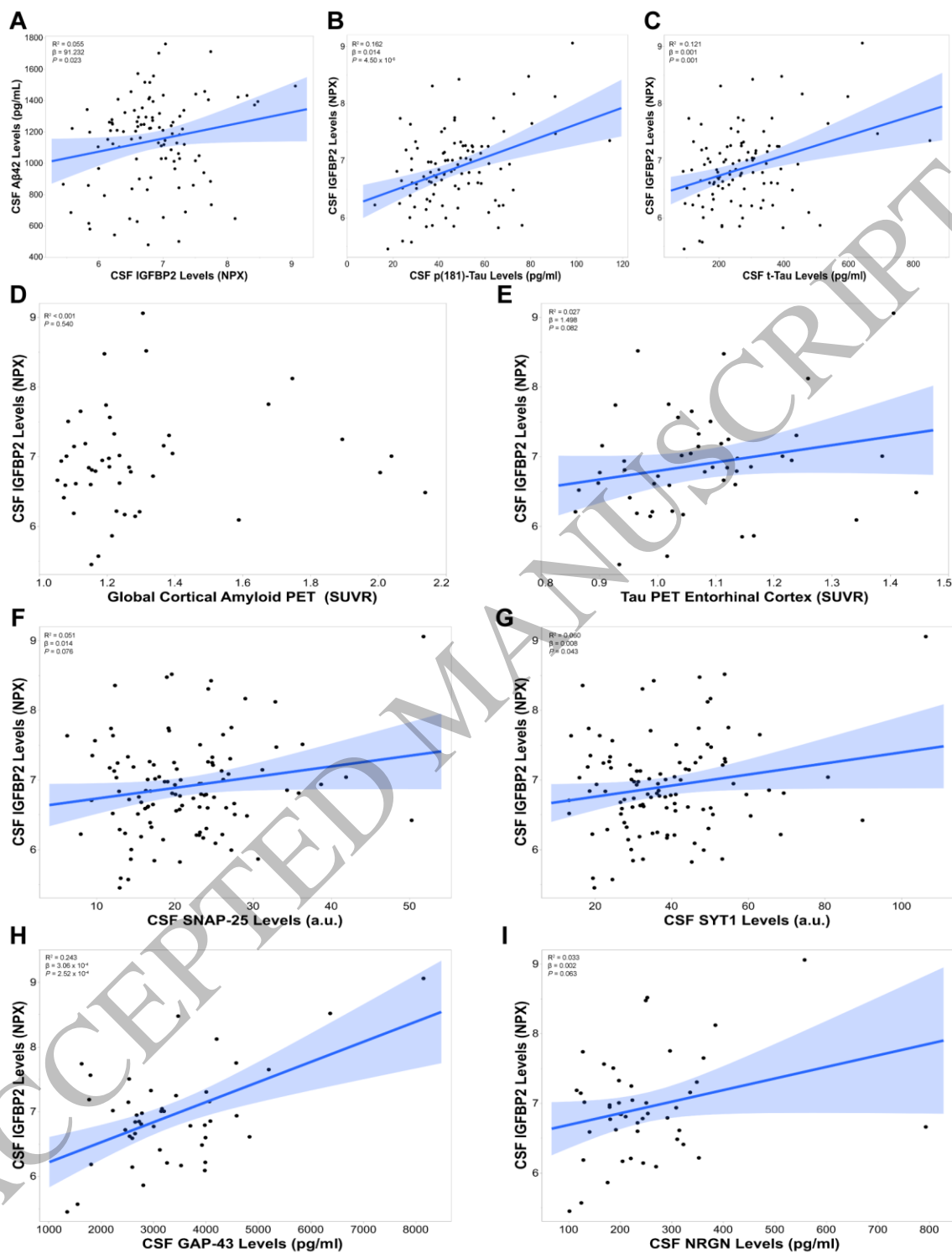
Figure 1
159x100 mm (x DPI)
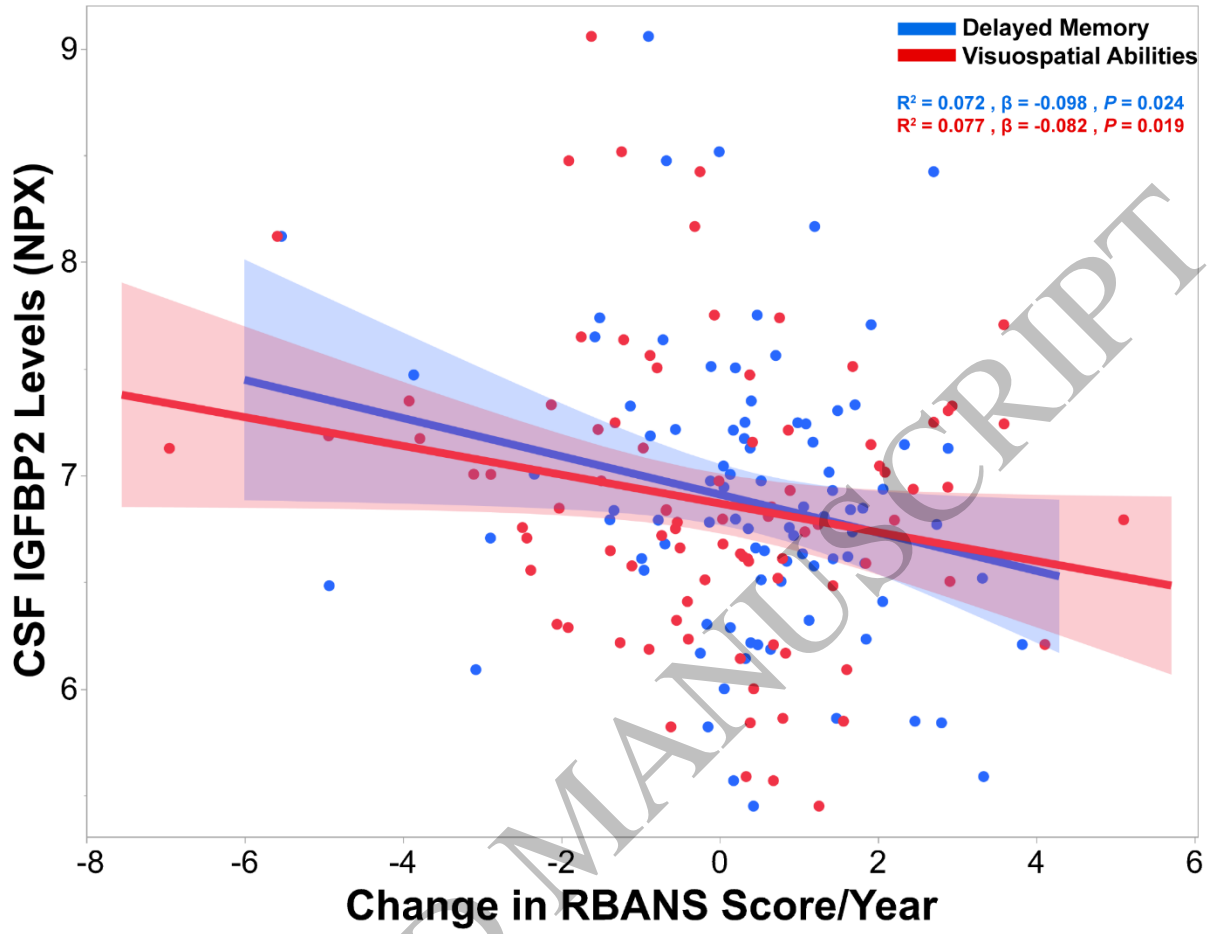
1

2 *Figure 2*
3 *150x198 mm (x DPI)*

4

Figure 3
159x124 mm (x DPI)

1

2

3

4

A

CSF IGFBP2 Levels (NPX)

Left Hemisphere
Right Hemisphere

R² = 0.117 , β = -39.720 , *P* = 0.082
R² = 0.088 , β = -1.193, *P* = 0.962

Entorhinal Cortex Volume (% of ICV)

B

CSF IGFBP2 Levels (NPX)

Left Hemisphere
Right Hemisphere

R² = 0.121 , β = -0.628 , *P* = 0.064
R² = 0.128 , β = -0.709 , *P* = 0.039

Piriform Cortical Thickness (mm)

C

CSF IGFBP2 Levels (NPX)

Left Hemisphere
Right Hemisphere

R² = 0.153 , β = -1.253 , *P* = 0.008
R² = 0.098 , β = -0.464 , *P* = 0.315

Inferior Temporal Gyrus Cortical Thickness (mm)

D

CSF IGFBP2 Levels (NPX)

Left Hemisphere
Right Hemisphere

R² = 0.144 , β = -1.369 , *P* = 0.014
R² = 0.116 , β = -0.959 , *P* = 0.090

Middle Temporal Gyrus Cortical Thickness (mm)

1

2
3

Figure 4
159x136 mm (x DPI)

4

A

B

C

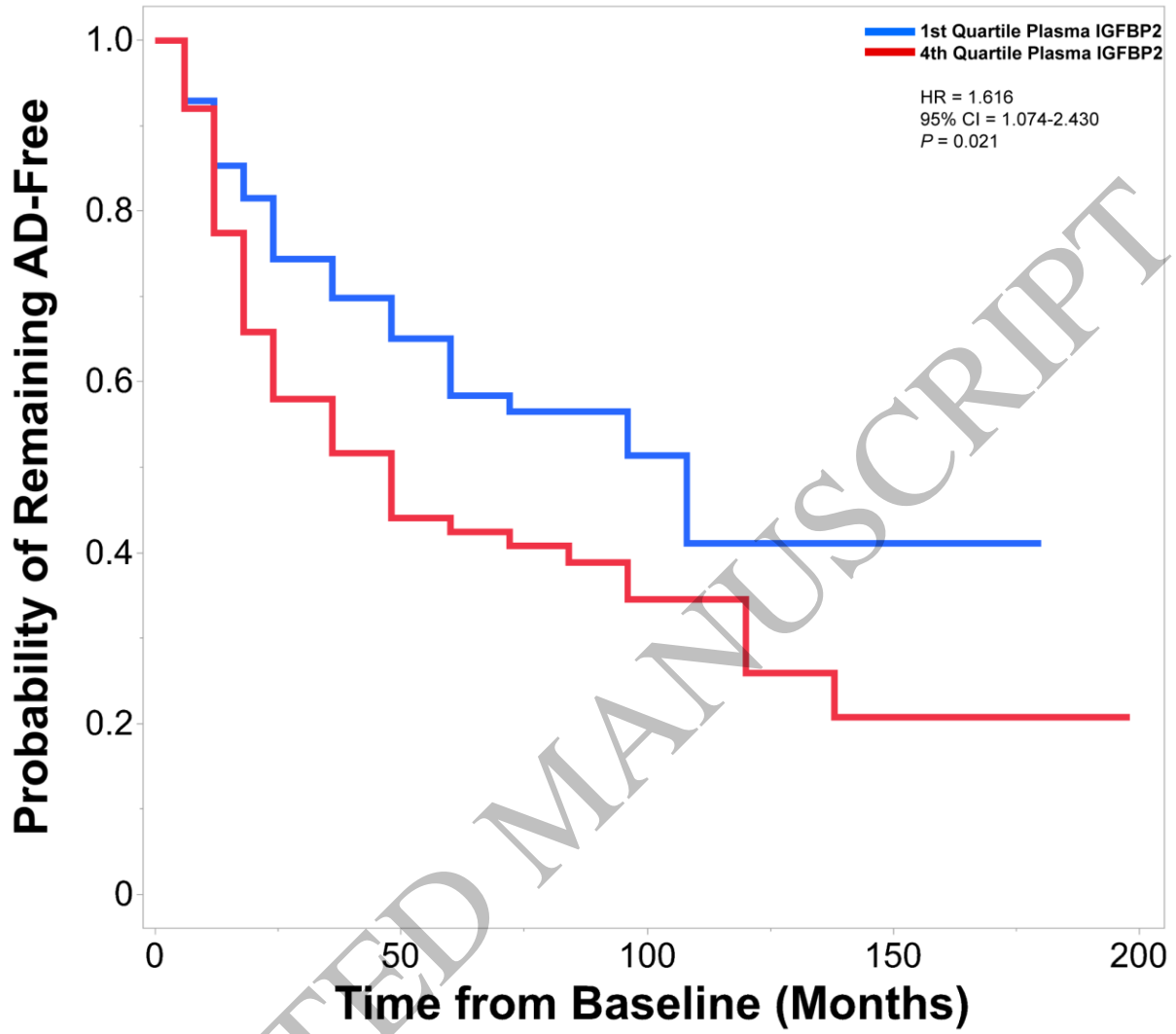*Figure 5*
159x180 mm (x DPI)

44

Figure 6
159x142 mm (x DPI)

1
2
3
4

A

B
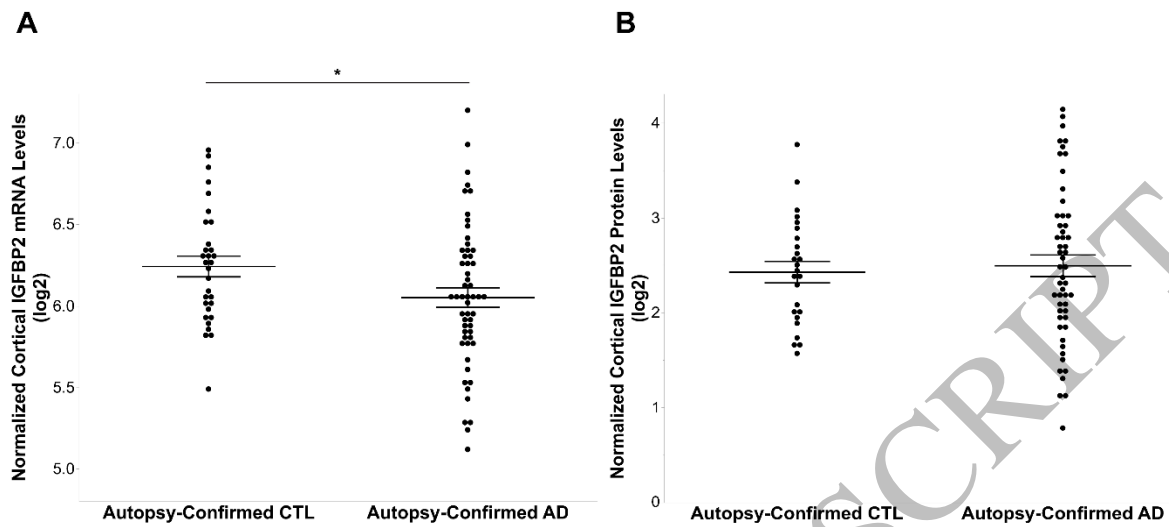
Figure 7
159x71 mm (x DPI)

1
2
3
4

1 **Table 1 Baseline Participant Demographics**

	PREVENT-AD	ADNI-1			QFP	
	CU	CU	MCI	AD	CU	AD
N Sample	109	58	395	111	31	55
Mean Age, Years (SD)	62.60 (5.43)	75.11 (5.77)	74.73 (7.40)	74.73 (8.08)	77.39 (11.37)	80.71 (6.39)
N Female (%)	76 (69.72)	28 (48.28)	140 (35.44)	47 (42.34)	11 (35.48)	23 (41.81)
N *APOE* ε4+ (%)	43 (39.44)	5 (8.62)	210 (53.16)	75 (67.57)	9 (29.03)	32 (58.18)
Mean BMI, kg/m^2 (SD)	27.11 (4.47)	27.02 (4.12)	26.09 (3.97)	25.59 (3.82)	-	-
Mean HbA1C, % (SD)	5.40 (0.40)[a]	-	-	-	-	-
Mean Systolic BP, mmHg (SD)	120.20 (13.85)	131.41 (17.65)	132.79 (18.14)	135.05 (17.11)	-	-
Mean Education, Years (SD)	14.88 (2.94)[b]	15.67 (2.78)	15.64 (3.04)	15.09 (3.21)	-	-
N Amyloid Positive (%)	37 (33.94)	21 (36.21)	205 (51.90)	91 (81.98)	0(0)	55 (100)
Mean CSF Aβ$_{42}$, pg/mL (SD)	1145.73 (277.62)[c,d]	250.85 (21.08)	163.48 (52.90)	142.56 (39.32)	-	-
Mean CSF p$_{181}$-tau, pg/mL (SD)	46.83 (18.00)[c,d]	21.07 (8.43)	36.15 (19.32)	42.05 (19.96)	-	-
Mean CSF t-tau, pg/mL (SD)	273.09 (129.97)[c,d]	63.62 (21.76)	102.33 (59.78)	120.47 (56.58)	-	-
Mean CSF IGFBP2, NPX (SD)	6.89 (0.67)	-	-	-	-	-
Mean CSF IGFBP2, ng/mL (SD)	-	100.85 (15.85)	104.93 (18.87)	103.02 (18.76)	-	-
Mean Plasma IGFBP2, log$_{10}$ (SD)	-	1.88 (0.20)	1.99 (0.23)	1.91 (0.12)	-	-
Mean Global Aβ, SUVR (SD)	1.30 (0.27)[e]	-	-	-	-	-
Mean Tau metaROI, SUVR (SD)	1.17 (0.07)[f]	-	-	-	-	-
Mean Cortical IGFBP2, log$_2$ (SD)	-	-	-	-	2.43 (0.56)[g]	2.50 (0.83)[g]
Mean Postmortem interval, h (SD)	-	-	-	-	30.03 (19.85)	21.07 (10.36)

2 PREVENT-AD, PResymptomatic EValuation of Experiment or Novel Treatments for Alzheimer's disease; ADNI-1, Alzheimer's Disease
3 Neuroimaging Initiative; QFP, Quebec Founder Population (autopsy confirmed cases only, amyloid positivity dependent on plaque density); CU,
4 cognitively unaffected; MCI, mild cognitive impairment; AD, Alzheimer's disease; APOE ε4+, Apolipoprotein ε4 carriers; BMI, body mass index;
5 kg/m^2, kilograms per square meter; HbA1C, hemoglobin A1C; BP, blood pressure; mmHg, millimetres of mercury; CSF, cerebrospinal fluid; Aβ$_{42}$,
6 amyloid beta 42; p$_{181}$-tau, phosphorylated tau 181; t-tau, total tau; IGFBP2, insulin-like growth factor binding protein-2; NPX, Normalized Protein
7 eXpression; SUVR, standardized uptake value ratio; ROI, region of interest; h, hours; SD, standard deviation; N, sample size; pg/mL, picograms
8 per millilitre; ng/mL, nanograms per millilitre.
9 [a]107 participants had HbA1c values available.
10 [b]106 participants had RBANS (Total Score) values available.
11 [c]101 PREVENT-AD participants had CSF Aβ$_{42}$, p$_{181}$-tau and t-tau (pg/mL) values available.
12 [d]PREVENT-AD (Fujirebio Innotest ELISA) and ADNI (INNO-BIA AlzBio3 Immunoassay) used different assays to measure the core CSF AD
13 biomarkers, which explains the differences.
14 [e]46 PREVENT-AD participants had Global Aβ SUVR values available.
15 [f]49 PREVENT-AD participants had Tau metaROI SUVR values available.
16 [g]78 QFP participants had cortical IGFBP2 protein values available.
17